Aus der Klinik für Kardiologie und Angiologie

der Medizinischen Fakultät Charité – Universitätsmedizin Berlin

DISSERTATION

A Novel Method of Early Detection of Congestion in Heart Failure Using Bioimpedance on a Pig Model

zur Erlangung des akademischen Grades
Doctor medicinae (Dr. med.)

vorgelegt der Medizinischen Fakultät
Charité – Universitätsmedizin Berlin

von
Lawrence Mutwol
aus Marakwet, Kenia

Gutachter/in: 1. Priv.-Doz. Dr. P. Fotuhi

2. Prof. Dr. med. S. Felix

3. Prof. Dr. med. H. U. Klein

Datum der Promotion: 19.11.2010

Dedication

Dedicated to Lydia, Rebecca and Francis Mutwol.

TABLE OF CONTENTS

1. Introduction

1.1. Congestive Heart Failure

Heart failure is a complex clinical syndrome that can result from any structural or functional cardiac disorder that impairs the ability of the ventricle to fill with or eject blood (1). This results usually from an underlying disorder e.g. coronary artery disease and develops slowly, often over years. It is the end stage of many heart diseases which, if not treated in time, leads to reduction of quality of life, hospitalization or death.

Acutely decompensated heart failure patients have to be hospitalized to receive rescue therapy because of recurrent and acute episodes of the disease. These patients usually end up in the emergency room with respiratory and circulatory insufficiency. Congestive heart failure (CHF) is associated with an enormous human and economic burden (2, 3, 4). This is due to high mortality, progressive and prolonged morbidity and recurrent hospitalization.

1.2. Classification of Congestive Heart Failure

Systolic heart failure results from ineffective contraction leading to pulmonary edema. Diastolic heart failure results from ineffective relaxation leading to improper filling and systemic edema. This could be due to muscle stiffness and is usually accompanied by normal left ventricular systolic function.

Depending on the affected side of the heart, heart failure can also be classified into left and right heart failure. Left heart failure engorges the pulmonary venous system. It is characterized by dyspnea on exertion, orthopnea, paroxysmal nocturnal dyspnea (PNP), cardiac asthma, pulmonary edema, general weakness and dizziness. Physical exam usually reveals pulmonary rales and S3 gallop. Among the principal radiological signs are change in size and form, signs of pulmonary congestion and an increase in the basal diameter of the heart. Those associated with right heart failure are right atrial and ventricular enlargement, increase in size of the vascular pedicle, elevated diaphragm resulting from congestion hepatomegaly and pleural effusion. Right heart failure engorges the systemic venous system and is characterized by weight gain, ankle and leg edema, jugular venous distension and hepato-jugular reflux, ascites, liver and gastric

congestion, increased central venous pressure (CVP) and increased right ventricular end-diastolic pressure (RVEDP). A global heart failure comprises a generalized increase in the cardiac size and a reduction of the retro-sternal and retro-cardiac space. Heart failure can also be classified into acute heart failure, decompensated chronic heart failure and stable chronic heart failure. Notable as well is the classification used by the New York Heart Association (NYHA) I – IV. This is a classification according to severity as summarized in the table below.

Class	Patient Symptoms
Class I (Mild)	No limitation of physical activity. Ordinary physical activity does not cause undue fatigue, palpitation or dyspnea.
Class II (Mild)	Slight limitation of physical activity. Comfortable at rest, but ordinary physical activity results in fatigue, palpitation or dyspnea.
Class III (Moderate)	Marked limitation of physical activity. Comfortable at rest, but less than ordinary activity causes fatigue, palpitation or dyspnea.
Class IV (Severe)	Unable to carry out any physical activity without discomfort. Symptoms of cardiac insufficiency at rest. If any physical activity is undertaken, discomfort is increased.

Table 1: Summarizing the New York Heart Association (NYHA) classification of heart failure.

1.3. Epidemiology

Heart failure is a common condition with a crude age-adjusted incidence in the general population of one to five cases per 1000 people per annum. The crude prevalence is three to twenty per 1000 people of the general population (5). Men are affected earlier in life than women but the longer life expectancy of women makes the prevalence ratio one to one. Both the prevalence and mortality rates are twice as high for blacks as for whites in American studies. The death rate from heart failure rose by 64% from 1970 to 1990.

Prevalence	15 million cases worldwide (3) 3-20 per 1000 in general population (5) Approximately 4.7 million Americans affected (1, 3) 1.4 million < 60 years of age in the USA 2%, 5% and 10% of ages 40 – 59, 60 – 69 and > 70 respectively 1.5 – 2% of population in Germany (6)
Incidence	1-5 per 1000 per annum in the general population (5) Around 465,000 new cases annually in the USA (1, 3) Doubles with each decade of age (3, Framingham study) 1% per ≥ 65 years of age, 2-3% of ages 85-94 (3) Up to 80 years of age men ≥ women, thereafter women ≥ men (3)
Hospitalizations	First listed diagnosis in 875,000 hospitalizations in the USA Secondary diagnosis in 1.8 - 2.5 million hospitalizations in the USA 11.4 – 28.5 days of admission per patient in the UK (4) One third readmission within 12 months in the UK 4) One third readmission within 6 months in the USA (4)
Physician Visits	1.7 million (1980) - 2.9 million (1993) in the USA
Prognosis	Worse than most cancer forms, worse in men than women Up to 1:5 deaths per year Sudden death 6-9 times more likely than general population 70% rise in prevalence between 1985 – 2010 in the Netherlands (4)
Costs	1 – 2% of total health care (4, 6, 7) € 2.9 billion in Germany (8) $38.1 billion for in- and outpatient in the USA (1) $290 – 378 million in Sweden in 1996 (7) $500 million spent on drugs annually (AHA)

Table 2: Summarizing the epidemiology of heart failure.

The increase in incidence and prevalence of CHF can be attributed to different factors. The aging of the population is an important contributor although it is worth noting that there is still a high incidence and prevalence in age-matched groups. Other factors are the growing prevalence of diabetes mellitus and the modern sedentary life style. The reduced mortality rates from coronary heart disease (CHD) and acute myocardial infarction (AMI) could paradoxically increase incidence and prevalence of CHF because patients surviving CHD or AMI could end up with heart failure due to myocardial damage. This improved survival is the result of development and improvement of implantable devices, interventional cardiology, thrombolysis, intensive care medicine and more potent drugs e.g. ACE inhibitors and ß-blockers. The increase in hospitalization can be attributed to the inevitable progression of the disease, the rising incidence, incomplete treatment

during hospitalization, poor application of CHF management guidelines, non compliance with diet and drugs and failure to seek care (9).

1.4. Causes, Risk Factors and Etiology

The etiology of CHF in adults differs from that of children. Whereas adults develop CHF mainly as a result of rheumatic, hypertensive and arteriosclerotic causes; children normally develop it mostly due to congenital and rheumatic heart diseases (10). Other pediatric causes are primary myocardial disease, paroxysmal supraventricular tachycardia, acute glomerulo-nephritis, anemia and pericarditis.

Among the risk factors for CHF are hypertension and ECG-left ventricular hypertrophy by combined appearance of which the risk of heart failure is increased fifteen fold (4). Others include coronary heart disease, cigarette smoking, valvular heart disease, myocardial infarction (MI), diabetes mellitus types I and II, hyperlipidemia, myocarditis, cardiac arrhythmias, obesity, family history, cardiomyopathies, pericardial disease (e.g. constrictive pericarditis), salt rich diet, severe emphysema (right heart failure), hypercholesterolemia, old age, male sex and black race. Hyper- and hypothyroidism have also been described by some authors as possible risk factors. Whereas hyperthyroidism causes CHF especially in patients with pre-existing cardiac disease by inducing sinus tachycardia or atrial fibrillation, hypothyroidism diminishes cardiac performance and is associated with a poor prognosis in CHF (11). Survivors of early childhood cancers treated with doxorubicin, patients suffering from amyloidosis, thiamine deficiency and infections (HIV, viral, rheumatic fever, Chagas disease etc) are also at an elevated risk. Long term use of anabolic steroids such as testosterone is associated with an elevated risk of CHF. Acute myocarditis can cause a temporary but life-threatening heart failure. Other suggested risk factors include elevated plasma homocysteine levels (12) and retinopathy as a marker of microvascular pathology (13).

The development of heart failure occurs in stages. An index event (e.g. acute myocardial infarction, gene mutation, acute inflammation, hypertension, valvular heart disease etc.) triggers a structural remodeling of the heart. The clinical syndrome of heart failure (e.g. salt and water retention, edema, low cardiac output and systolic dysfunction) then occurs following this change of structure. Examples of structural remodeling reflecting disease

progress include myocyte hypertrophy, fibrosis, chamber dilatation, apoptosis, cell necrosis, neuroendocrine activation, cytokine release, increased wall stress and chamber dysfunction.

The causes of pulmonary edema are usually increased hydrostatic pressure (cardiogenic pulmonary edema) e.g. by pulmonary congestion in congestive heart failure and changes in capillary permeability (non-cardiogenic pulmonary edema) e.g. in sepsis (14). Clinical signs of edema develop after an increase of interstitial fluid of at least six times the normal value. In CHF, congestion leads to an increase of extra-cellular fluid volume (ECV). Pulmonary edema usually occurs progressively, starting with redistribution of vascular volume to superior parts of the lung, the preclinical interstitial edema, and clinical alveolar edema before the upper airways get filled with the frothy edematous fluid (15).

1.5. Symptoms, Diagnosis, Monitoring and Therapy

Symptoms of heart failure include dyspnea, tachypnea, orthopnea, paroxysmal nocturnal dyspnea, nocturia, edema (pulmonary and / or peripheral), coughing and wheezing, tachycardia, chronic fatigue, severe upper quadrant pain and abdominal fullness, nausea, vomiting and anorexia. The physical signs include rales, third heart sound and elevated jugular venous pressure.

Current diagnostic and monitoring procedures in congestive heart failure include chest X-ray, echocardiography, ECG, brain natriuretic peptide (BNP), pulmonary catheter, weight controls and, in more recent studies, bioimpedance.

Chest X-ray shows cardiomegaly and signs of pulmonary congestion. Kerley B lines (fine horizontal lines in lower lung segments) as well as alveolar and interstitial edema may also be visible. Pleural effusions are sometimes visible. Echocardiography may show reduced ejection fraction and eccentric ventricular hypertrophy. Electrocardiography (ECG) is usually non diagnostic but myocardial infarction and atrial fibrillations may precede acute decompensation.

Atrial natriuretic peptide (ANP) and BNP are released by stretching of atria and ventricles due to volume / pressure increase. Their quantities correlate with severity of heart failure with normal values being under 100 pg/ml and values of as much as 1000

pg/ml measurable during heavy decompensation. During acute heart failure, creatine kinase and Troponin can be tested to exclude myocardial infarction. Creatinine may be elevated and sodium reduced in heart failure.

Pulmonary catheter (Swan-Ganz) is used to differentiate between cardiogenic and non cardiogenic pulmonary edema in suspected heart failure patients. Alveolar pulmonary edema is seen by wedge pressures around 20-25 mmHg and interstitial edema over 25 mmHg (16). The fact that not all CHF patients show clinical signs despite elevated filling pressures and that these parameters are non quantifiable, demonstrates the need of a more precise method of determination in order to make more accurate diagnosis and therapy possible. The current method of pulmonary catheter is invasive, requires inpatient care and is generally not yet routinely used. A reliable, non invasive, less expensive and quantifying alternative is desirable. The aim of this work seeks the fulfillment of such a need.

Other diagnostic procedures in heart failure described in literature include nuclear angiography, magnet resonance imaging and coronary angiography. These diagnostic and monitoring procedures have two major setbacks. They are incapable of predicting preclinical decompensation and thus leading to the condition being diagnosed so late that hospitalization is mandatory. Secondly, they are not routinely usable in the home setting by heart failure patients. They also require specialized trained health personnel and greatly interfere with the patient's activities of daily life.

Therapy in patients with high risk of heart failure targets the eradication of risk factors such as hypertension, coronary heart disease and diabetes mellitus (primary prevention). The early eradication of risk factors delays or even prevents the onset of heart failure (5, 17, 18).

Patients with structural heart disease (e.g. previous myocardial infarction (MI), LV systolic dysfunction and asymptomatic valvular disease) but without symptoms of heart failure benefit further from post MI therapy, ACE inhibitors and beta blockers (19, 20, 21). This can be widened in patients with structural heart disease with diuretics and digitalis. Patients with refractory heart failure may also require mechanical assist devices, heart transplantation, continuous intra-venous medication, hospice care, biventricular

pacing, vessel dilatation or bypass measures and stem cell therapy. Another recently postulated possible form of therapy is the inhibition of 5-phosphodiesterase (PDE5) (22).

1.6. Bioimpedance

Bioelectrical impedance (bioimpedance) is the change in electrical resistance of biological tissues. In this thesis, the term bioimpedance and impedance are used synonymously and abbreviated to Z.

Electrical current travels through most conductive parts of tissue, such as the blood-filled aorta. Changes in impedance resulting from pulsatile changes in volume and velocity of aortic blood are inversely proportional to stroke volume and generally reflect left ventricular changes.

$$CO = SV \times HF$$

Formula demonstrating the relationship between cardiac output (CO), stroke volume (SV) and heart frequency (HF).

Bioimpedance can give information about physiological processes such as ventilation and circulation. It consists of a basal impedance value Zo and a varying value Zt. The basal impedance is the electrical resistance independent of physiological changes. It is the result of structural and anatomical differences affected by factors such as age and sex (15, 23). The varying value is the result of Z fluctuations resulting from physiological changes. Zt value is of more relevance to our experiments. Some investigators have suggested that Zt is affected by both Zo and peak aortic flow (14, 23).

A three element equivalent circuit consists of an active resistance R (representing extra-cellular and inter-cellular fluid), a parallel branch characterizing the cells, capacitors (representing the cell membrane) and the serially connected intracellular fluid (24).

Different body tissues show differences in their electrical properties and resistances, modulated by the frequency of the electrical current being applied (see results figure 15). This has also been confirmed by the work of other investigators (25, 26). At frequencies

below 1 kHz, cells act as insulators and conductance here is based on fluid conduction. At frequencies of 10-500 kHz, dielectric properties of the lung are supposed to be due to capacitive charging of alveolar structures. At frequencies above 100 kHz, the dielectric properties of the lung are supposedly due to polarization of erythrocyte membranes in the alveolar capillaries. Thus, impedance is at such high frequencies is no longer selective.

Tissue	ρ[Ωm]	Remarks	Reference
Cerebrospinal fluid	0.7		Barber and Brown, 1984
Blood	1.6	Hct = 45	Geddes and Sadler, 1973
Plasma	0.7		Barber and Brown, 1984
Heart muscle	2.5	longitudinal	Rush, Abildskov, and McFee, 1963
	5.6	transverse	
Skeletal muscle	1.9	longitudinal	
	13.2	transverse	Epstein and Foster, 1982
Lung	11.2	longitudinal	
	21.7	circumferential	Schwan and Kay, 1956
Fat	25	radial (at 100 kHz)	Rush, Abildskov, and McFee, 1963
Bone	177		Geddes and Baker, 1967

Table 3: Summarizing selected tissue resistivities. Adapted from Malmivuo et al. (27)

The resistance of a system, R is proportional to resistivity, and inversely proportional to its cross-sectional area.

$$R = \rho \frac{L}{A}$$

Formula depicting relationship between resistance (R), resistivity (ρ), length (L) and cross sectional area (A).

The total resistance of a system in parallel can be calculated as:

$$\frac{1}{R_{total}} = \frac{1}{R_1} + \frac{1}{R_2} + \ldots + \frac{1}{R_3}$$

Formula depicting the total resistance of a system in parallel. R1, R2 and R3 represent resistances (impedances).

Based on the preceding formula, the partial resistance with the smallest value has the biggest effect on the total resistance. Blood conductance is about seven times that of lung (28). This means that blood resistance is only about one seventh that of the lung (conductance = 1 / resistance). Since lung and blood could be considered as on a parallel circuit, the total impedance here would be greatly determined by the blood path. This would make the aorta the preferred conduction route. Changes in conductivity also result from alignment of planes of erythrocytes parallel to the main axis of the aorta. This results from changes in blood velocity which increases conduction during the initial phase of ejection. Distension of aorta, hematocrit, complex path of conduction and correcting cyclical changes in lung gas volumes also play a role.

Bioimpedance is measurable with two electrodes. This configuration is usually unfavorable due to the development of a bi-layer charge around the implanted current source leading to a high electrode polarization effect. The tetra-polar electrode configuration is less polarized and is therefore generally favored. To enable a uniform impedance to be measured, the electrodes should remain as fixed as possible. Experience has also shown that, unlike electrodes placed in the extremities as is done in some forms of impedance cardiography, electrodes placed on the chest are more sensitive in measuring changes in lung volumes (29). The impedance generator injects a small electric current (100 μA) at a high frequency. Because the current is constant, changes in voltage across biological tissues is the result of changes in impedance in these tissues.

Other indications for thoracic electrical bioimpedance reported in literature include differentiation of cardiogenic from pulmonary causes of dyspnea, optimization of atrioventricular interval in patients with A/V sequential pacemakers, inotropic therapy

monitoring in heart failure patients who have chosen to die at home or those awaiting heart transplants, evaluation of post-transplantational heart rejection and optimization of fluid management in patients with congestive heart failure.

1.7. Telemonitoring

Telemonitoring allows the monitoring of physiological variables measured in patients at home by physicians and caretakers by making use of standard telecommunication technology e.g. telephone, cable etc. This would allow the close monitoring of heart failure patients and facilitate early intervention in case of worsening and so prevent hospitalization. Consequently, rates of admission to hospital would be reduced and discharge accelerated. Observational studies suggest that telemonitoring could be used alone or together with other care programs. In a review of 18 observational studies and six randomized controlled studies with heart failure patients, Louis et al. (30) described a significant reduction of hospital days and occupancy where telemonitoring was used. There was also a high rate of acceptance and compliance by patients. Two randomized trials suggested reduction in readmission and length of hospitalization as well as early detection of deterioration. One trial showed reduction of mortality in six months and another reduction in readmission. However, one study showed no significant difference between the telemonitoring and the standard monitoring group.

The development of telemedical care has been influenced by rising hospital costs, advances in diagnostics, its comparatively low cost, patient friendliness of the equipment, increase in aging multi-morbid population, comfort of homecare and rapid advances in telecommunications technology. The technology supporting telemedicine includes the availability of mechanical cardiac assist devices, portable infusion pumps, portable cardiac and hemodynamic monitors and telemonitoring. The epidemiological and financial significance of heart failure predicts home care as a price-lowering solution with a good potential. The reliability of this technology is yet to be proved, but Scherr et al. (31) described a high compliance, 83% success in data transfer, 98% stability in the telemonitoring system and ease of use by both patients and health care professionals in a mobile-phone surveillance of home-based patients. There is good evidence that home based telemedical care can reduce readmission rates and hospitalization length in heart

failure (30, 32). It also has the potential of long-term telemonitoring (33). Currently, the monitoring of the patient at home is based mainly on physical assessment findings, daily weighing and functional status. Hemodynamic indices that reflect cardiovascular status have proved to be more reliable than physical signs and symptoms and chest radiographs or even ECG. Telemonitoring has the capacity to optimize therapy, promote appropriate use of financial resources, enhance quality of care of the patient and avoid risks associated with hospitalization. Improvement of quality of life results through reduction in number of visits to healthcare institutions for evaluation and adjustment of medicine, reduction of regular right heart catheterization in hospital, higher functional status due to right timely medical titration and an optimized hemodynamic status.

Bioimpedance in relationship with telemedicine offers a possible monitoring solution for home-based heart failure patients. Telemonitoring allows monitoring of physiological variables measured on patients at home by physicians and caretakers by making use of standard telecommunication technology e.g. telephone, internet etc. The viability of both telemedicine in monitoring patients at home and bioimpedance in monitoring heart failure has appeared separately in several publications.

2. Aim

The aim of this study was to determine if local subcutaneous bioelectrical impedance (Z) correlates with respiration parameters (tidal volumes and respiration rates), fluid overload (fl) and cardiac output (CO); and could therefore serve as an indicator for changes in hemodynamic status. Heart failure is associated with a reduction of cardiac output and an increase in lung and peripheral fluid congestion. Changes of Z around the lungs during heart failure could therefore be measurable during lung fluid congestion.

3. Materials and Methods

3.1. Measurements Overview

The experiments were carried out on eight female pigs weighing between 29 and 42 kg. Bioelectrical impedance (bioimpedance, Z) was measured by implanting a pacemaker-sized electrode array subcutaneously, hereafter referred to as SubQ array (SubQ array, Medtronic Inc, MN). A SubQ array was implanted in subcutaneous pockets on the lateral sides of each pig's chest. A surgical approach similar to that used for pacemaker implantation is used to place electrodes in the heart and the device in the subcutaneous pocket. Bipolar pacemaker leads were implanted in the right ventricles (RV) and right atria (RA). The pigs were thereafter left for 9-12 days to allow fixation of the arrays and leads. After the fixation, a follow up procedure was done, whereby unipolar pacemaker leads were implanted in the coronary sinuses (CS) and follow up measurements made.
Three types of impedance measurements were made:

- Measurements of absolute bioimpedance
- Measurements of change in bioimpedance over time in relation to respiration
- Measurements of change in bioimpedance over time in relation to heart action.

3.2. Equipment

The following equipment was used for the data acquisition and analysis per animal:
A-V pacing system analyzer model 5311 (PSA, Medtronic Inc, MN)
SubQ electrode array (Medtronic Inc, MN)
Biopac system (Biopac Systems Inc, CA) consisting of:

Electrical bioimpedance amplifier EBI100C
MP100A-CE Biopac systems drive and interface cables
Five DA100C general purpose transducer amplifiers (four for pressures and one for airflow)
Four TCI105 phone jack modules for pressure transducer
TSD117 air flow transducer
ECG100C electrocardiogram amplifier
Three ECG leads

MEC111C protected touch-proof input extension cable for ECG

UIM100C universal interface module

AFT6 volume calibration syringe

One unipolar and two bipolar pacemaker leads (Medtronic Inc, MN)

Three pressure transducers (Hospira Inc, IL)

A XCALIBER transducer calibration system (Gould, CA)

Eight and seven French vessel sheaths (Johnson and Johnson, NJ)

A pig-tail catheter (Johnson and Johnson, NJ)

Swan-Ganz catheter (Edwards Lifesciences, Irvine, CA)

A continuous cardiac output (CCO) monitor (Edwards Lifesciences, Irvine, CA)

Moisture filter for air flow transducer (Smiths Medical, NH)

One interface box (custom-made)

Fluoroscopy equipment (General Electric Company, WI)

2363 BRC Medtronic Z generator (Medtronic Inc, MN)

The SubQ Array

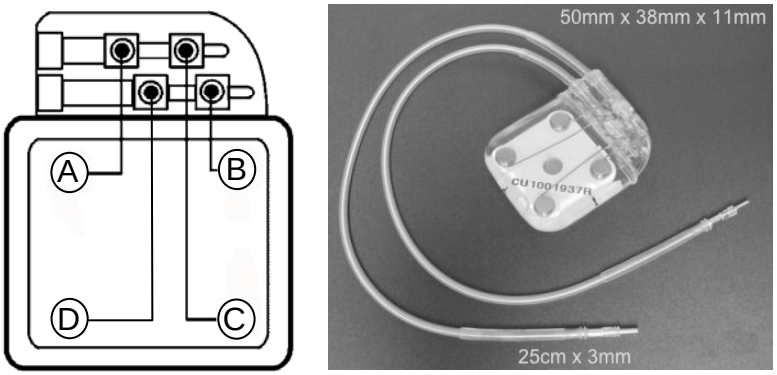

Figure 1: Schematic picture of the array (left) with surface electrodes depicted as A, B, C and D. On the right picture the array with attached electrodes.

The 5 x 3.8 x 1.1 cm measuring SubQ array consists of four surface electrodes (depicted above as A, B, C and D). Two of these electrodes are used to apply current and the other two to measure the resulting voltage. From the measured current and voltage, the

impedance is derived by the EBI100C. Two headers are connected to the device on one side and over connecting wires to the EBI100C on the other during measurement.

3.3. Medicine / Fluids

The following drugs and fluids were used during and after the procedure:
Metoprolol 0.08 (0.18) mg/kg body weight (BW)
Verapamil 0.08 (0.18) mg/kg BW
Calcium chloride, 18-36 mg/kg BW
Heparin 5000IE
Telazol 6.6 mg/kg BW
Furosemide 0.4 mg/kg BW
HAES (6%) ml/kg
Saline (0.9%) 2ml saline/kg
Isoflurane (1.5 – 2%)
Buprenorphine (0.01- 0.05 mg/kg) where necessary
Epinephrine, atropine, norepinephrine where necessary

3.4. Computer Programs

The following software was used:
AcqKnowledge® (Biopac Systems Inc, CA)
National Instruments Labview®7.0 (National Instruments, Texas)
Diadem (National Instruments, Texas)
Microsoft® Office (Microsoft Inc, USA)
zsCompare (Zizasoft, CO)
Adobe Photoshop (Adobe Systems Incorporated, CA).

3.5. Procedure

The procedure involved two operations per pig. The first operation involved the implantation of the SubQ arrays and electrodes with a subsequent period for encapsulation resulting from formation of adhesions. The second operation involved implantation of an extra electrode and taking of measurements.

3.5.1. Implantation

Anesthesia

Anesthesia was induced with a Telazol dose of 6.6 mg/ kg body weight (mg/ kg BW) intra muscular (IM) and maintained by 1.5% - 2.5% inhalational isoflurane following endotracheal intubation. Prior to and during the procedure the heart rate, blood pressure, respiratory rate, O_2 saturation, body temperature and spontaneous movements were monitored. Extubation was done following respiratory sufficiency and the recurrence of the lid reflex. Buprenorphine (0.01- 0.05 mg/kg) was administered intra-venously (IV) as an analgesic where necessary.

ECG Leads

A lead II ECG was recorded. Shaving and cleaning of the hairy skin before electrode placement was necessary to record a stable signal.

Implantation of SubQ Arrays

In this experiment, all surgical procedures were conducted using the aseptic technique. A scalpel and a pair of blunt-tipped dissecting scissors were used to form a subcutaneous pouch on the left side of the pigs´ chest where the SubQ arrays were inserted. Following insertion, the SubQ arrays were then secured underneath the skin of the thorax to the body wall with non absorbable sutures and the leads connected to extension cables from the EBI100C for measurement. Suturing was used for closure of skin incisions. Sutures were removed 7- 10 days post operatively.

Catheterization and Electrode Implantation

Both ipsilateral jugular veins and a carotid artery of the pigs' right side were accessed during the implantation. The vessels are located deep within the neck musculature. Their surgical approach is along an imaginary line joining the medial part of the mandible and the point of the shoulder, almost parallel the cervical vertebrae. The dissection was made between sternocephalic and brachiocephalic muscles. The external jugular vein is first to be found. The sternocephalic muscle is the guiding muscle for the internal jugular vein

which lies on its dorsal surface. This was approached by blunt dissection along the muscle after securing the external jugular vein. The sheath was then carefully opened and the vein and the carotid artery retracted outwards towards the external vein for catheterization. The vessels where permanently occluded cranially.

The Seldinger´s technique was used to place a 7 French vessel sheath in the artery and 8 French sheaths in the veins for placement of catheters and electrodes. A pigtail catheter was placed over the carotid artery in the left ventricle for measurement of left ventricular end-diastolic pressure and left ventricular end systolic pressure (LVEDP and LVESP). Over one of the jugular veins a Swan-Ganz catheter was inserted into the pulmonary artery and the continuous cardiac output (CCO), pulmonary artery pressure (PAP) and pulmonary capillary wedge pressure (PCWP) were measured. Two standard bipolar pacemaker leads were implanted over the other jugular vein in the apex of the right ventricle and in the right atrium. Catheter and electrode placement was done under fluoroscopy.

3.5.2. Follow up

The SubQ arrays and the pacing leads were then left in the animal for 9-12 days for adhesive fixation. Follow up vessel access was done on the contralateral side similarly as with the implantation. Additionally, a standard unipolar pacemaker lead was placed over the jugular vein into the coronary sinus. Measurement taking followed subsequently.

3.5.3. Study Set-up

The SubQ arrays and the pacemaker leads were connected to the EBI100C. Connection wires were used to link the Swan-Ganz catheter to the CCO monitor, the latter being connected to the general purpose amplifier (DA100C). The TSD117C airflow transducer was linked on one side to the pig and on the other to both the ventilator and the DA100C. Other DA100Cs were connected to the pressure transducers. The ECG leads were joined over an elongation wire MEC111C to the ECG100C. The amplifiers (DA100Cs, ECG100C and EBI100Cs) were all connected in series with each other and with the UIM100C (the latter being last in the series because it has one connectable end) by fitting their male / female ends. The UIM100C was then connected to the MP100A-CE Biopac

systems drive which was linked over connecting wires to the computer. The Medtronic impedance generator was connected to the UIM100C.

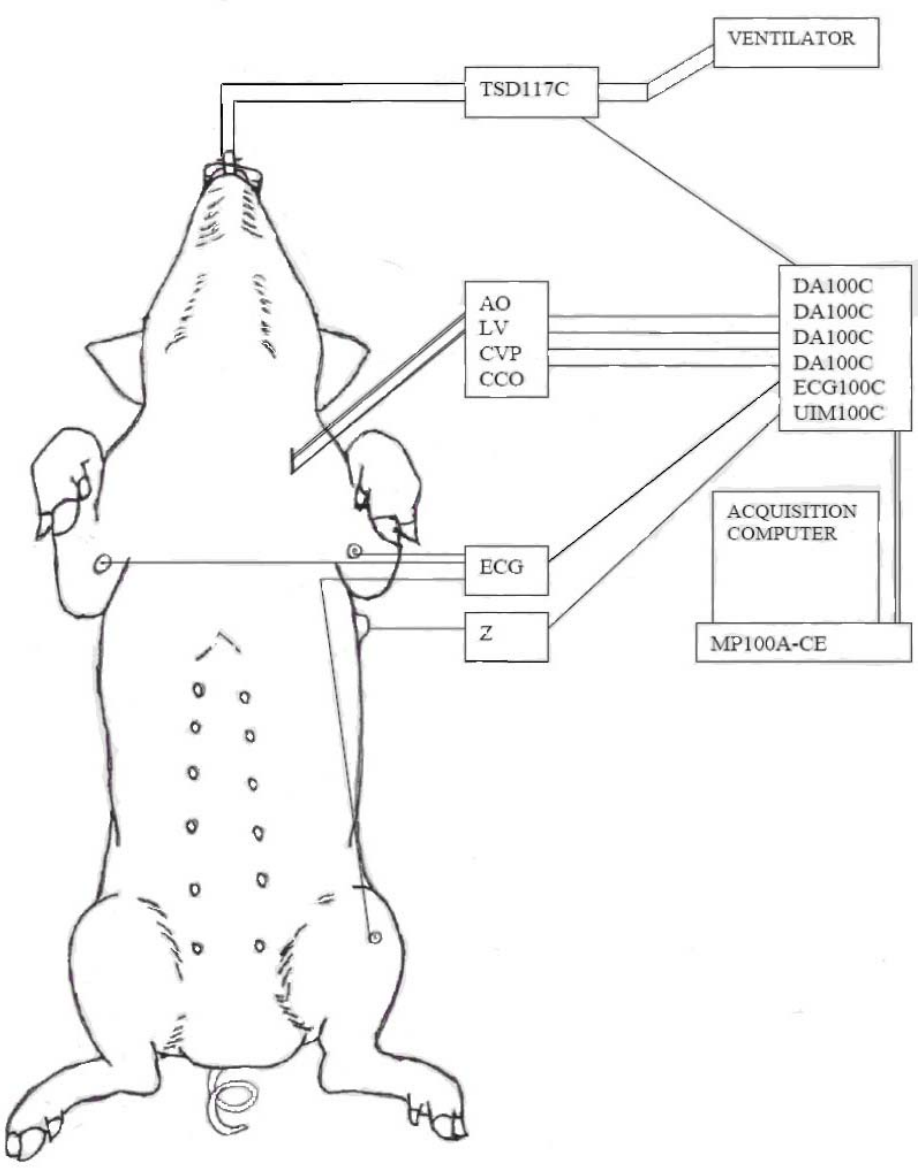

Figure 2: The figure depicts the study set-up (pacemaker leads not shown). The transducers for the different measurements were connected between the pig and their respective amplifiers in the Biopac system. Attached to the Biopac system is the acquisition laptop. AO=Aortic Pressure, LV= Left Ventricular Pressure, CVP= Central Venous Pressure, CCO= Continuous Cardiac Output and Z=Impedance. For the abbreviations of the Biopac system please refer to section 3.2 describing used equipment.

3.5.4. Alteration of Hemodynamic and Ventilation Parameters

Metoprolol and Verapamil (0.18 mg/kg body weight each) as well as saline and 6% HAES (4 ml/kg body weight each) were applied intravenously to achieve acute fluid overload and pulmonary congestion. The amount of medication and fluids administered was adjusted according to the individual animal response. Fluid overload was induced by reducing the stroke volume in two steps by 25% each step (later referred to as fluid overload one (fl1) and fluid overload two (fl2) respectively). After measurements, the fluid retention was counteracted by administration of 0.4 mg/kg BW furosemide and 16-32 mg/kg BW calcium chloride. Atropine / epinephrine / nor epinephrine were used to stabilize hemodynamic parameters where necessary.

A positive pressure ventilator was used to adjust tidal volumes and respiration rates. Tidal volumes were modified to find out if stepwise changes reflect a corresponding change in impedance values. Three sets of tidal volumes and corresponding respiration frequencies were used in all the pigs: A high tidal volume of 650 ml was combined with a low breath frequency of 9 breaths/min, a medium tidal volume of 450 ml with a medium frequency of 13 breaths/min and a low tidal volume of 360 of ml with a high breath frequency of 19 breaths/min. Target was maintenance of respiratory minute volume of about 5.8 liters.

	Tidal Volume	Breath Rate
High	650 ml	9 breaths/min
Medium	450 ml	13 breaths/min
Low	360 ml	19 breaths/min

Table 4: Summarizing tidal volumes and breath rates used in each fluid overload level.

3.6. Measurement Configurations

Two types of bioimpedance measurements were done: Absolute bioimpedance and change in bioimpedance.

The absolute bioimpedance measurement was done by use of a Medtronic pacing system analyzer (PSA). Measurements of change in bioimpedance were conducted using an electrical bioimpedance amplifier EBI100C with a frequency of 12.5 kHz and a sampling

rate of 200 per second. Sample recordings were also made in 4 and 100 kHz with 2363 BRC Medtronic Z generator and the EBI100C, respectively.

For both types of bioimpedance measurements, the fluid content in the lungs was measured in baseline and two progressive fluid overload stages. Ventilation was done with three levels of lung tidal volumes: Low, medium and high in each fluid overload level.

	Baseline	Fluid Overload 1	Fluid Overload 2
Absolute Z	X	X	X
Change in Z	X	X	X

Table 5: Summarizing the basic measurement protocol for absolute and change in bioimpedance. These measurements were repeated in low, medium and high tidal volumes.

3.6.1. Absolute Bioimpedance Measurement

The A-V pacing system analyzer (PSA) was placed laterally on the pigs´ chest and absolute bioimpedance measurements conducted. This was done with direct current generated from the battery powered PSA. Measurements were conducted at baseline, fluid overload one (fl1) and fluid overload two (fl2); and at the different tidal volumes levels: Low, medium and high (see table 4 for the basic measurement protocol).

3.6.2. Subcutaneous Measurement of Change in Bioimpedance

The subcutaneous bioimpedance measurement was carried out on the pigs' lateral chest walls on the left sides to measure the respiratory derived change in bioimpedance during baseline, fl1 and fl2 in low, medium and high tidal volumes. Measurements were done using the surface electrodes of the SubQ arrays. These measurements were therefore made from the lateral surface of the lungs only. The basic protocol described in table 4 was used.

3.6.3. The Intra-cardiac Measurement of Change in Bioimpedance

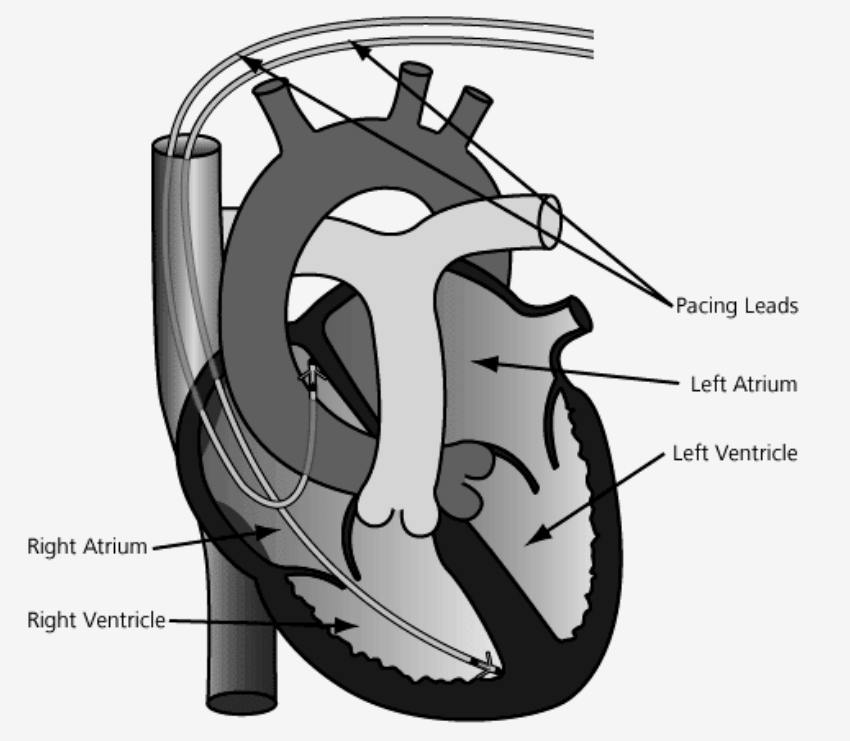

Figure 3: Showing the measurement of the intra-cardiac bioimpedance using pacemaker leads. One bipolar lead was placed in the RA, another one in the RV and a unipolar one in the CS (CS lead not shown). Image adapted from http://www.immnet.com/images/issues/2004/June/Focus_Tour_pacemaker.gif

For this configuration, all measurements were made exclusively with intracardiac electrodes in order to measure impedance changes derived from the cardiac cycle. One bipolar lead was placed in the right atrium, one in the right ventricle and a unipolar in the coronary sinus. The measurements were made from the right ventricular ring and right atrial ring to the coronary sinus tip and right atrial tip (see table below 2nd column).

	RV Ring – RA Ring CS Tip – RA Tip	RV Ring – SubQ RV Tip – SubQ	RV Ring – SubQ CS Tip – SubQ
Baseline	X	X	X
Fluid Overload 1	X	X	X
Fluid Overload 2	X	X	X

Table 6: Summarizing the basic measurement protocol for change in bioimpedance. These measurements were repeated in low, medium and high tidal volumes.

3.6.4. Intra-cardiac to Subcutaneous Measurement of Change in Bioimpedance

This configuration measured the change in bioimpedance from lateral and medial surfaces of the lung. Electrodes on pacemaker leads were placed intra-coronary and the circuit was completed by two electrodes from the SubQ array (see table 6, 3th and 4th columns). Two measurement types were done:

- Measurements were done between two electrodes in the RV and two of the SubQ array.
- Measurements were done with one electrode in the RV, one in the CS and two from the SubQ array.

3.7. Data Acquisition

3.7.1. Setting up Channels

Acquisition channels were set by awarding each measurement a channel number corresponding both to the hardware and software of the Biopac system. The hardware channels were set by manually adjusting a button at the top surface of the amplifiers to the desired channel number, which would then be automatically recognized by the UMI100C. The channel of the cardiac output monitor and the Medtronic impedance generator were set by connecting the output cables to the desired channel outlet number on the UIM100C which would then be automatically recognized by the software as assigned channel numbers.

On the AcqKnowledge software, the channels were set by activating sample channels. These sample channels were labeled and matched to the corresponding channel numbers

on the hardware. They were activated as acquisition channels with a single mouse click on “acquire” button in the acquisition window.

3.7.2. Pressure Calibration and Zeroing of Channels

The calibration of pressure channels involved applying two values of pressure on a pressure transducer which is connected to a transducer calibration system. The first value was a value around zero and the second one around 100 mmHg. These two values were then read off from the calibration device and fed to the computer.

The airflow channels were calibrated by using the volume calibration syringe AFT6, which had a capacity of 600 ml. The syringe was filled to maximum capacity and completely emptied. Both values were then fed on the inflow and outflow channels respectively i.e. 600 ml and 0 ml. The channels were zeroed by turning the respective screw head on the amplifiers with a slotted tip screw driver until the signal was aligned to the zero line. This sets zero as the base value when there is no incoming signal.

3.7.3. Acquisition

Data was acquired at the rate of 200 samples per second and saved as single continuous Acqknowledge files. Measurements were gated to QRS complex and end expiration. Every change in measurement configuration was indicated by placing a marker that can be activated and labeled on the software. Data collected on the different channels were:

- Bioelectrical impedance (Z)
- Cardiac output (CO)
- ECG
- Pulmonary capillary wedge pressure (PCWP)
- Pulmonary arterial pressure (PAP)
- Central venous pressure (CVP)
- Aortic pressure (AO)
- Left ventricular pressure (LV)
- Inspiration volume
- Expiration volume.

3.8. Analysis

Data analysis was done with three computer programs. The acquisition program AcqKnowledge was used to create text files from selected points of the raw data which were thereafter used by the Diadem and Labview software as described in the subsequent sections.

3.8.1. Creation of Text Files from Raw Data Using Acqknowledge

Segments of data with a length of fifteen to twenty seconds with a stable signal and low noise content were selected in each measurement configuration. This was done by highlighting the desired segment of the signal from where the computer picks its data. Thereafter, the text icon on the Acqknowledge program was clicked and the data deposited (Ctrl + D). The text files were then named and stored.

3.8.2. Visual Comparison of Data Using Diadem

With the Diadem program, segments of around 30 seconds were chosen in the impedance, left ventricular pressure, ECG and tidal volume channels. Data of the same fluid load level were then put on one scale for easier visual analysis and comparison. These were stored as JPG files and printed out for easier visual overview and comparison.

3.8.3. Actual Data Analysis with Labview

The main data analysis was done with the Labview program, a version specifically modified for this purpose. The first step involved choosing the desired channels (inspiration, ECG, impedance and left ventricular pressure channels) from the text files made before (see section 3.8.1) and clicking on the ´next´ button. The chosen channels appeared then on a general overview window which showed their entire plot. This window allowed the separation of good from noisy signals. Noisy sections of the curves were discarded. If an entire wave had a bad signal due to artifacts, then its entire run was skipped. This window also offered the possibility to magnify a wave segment, to filter and to invert the impedance wave vertically.

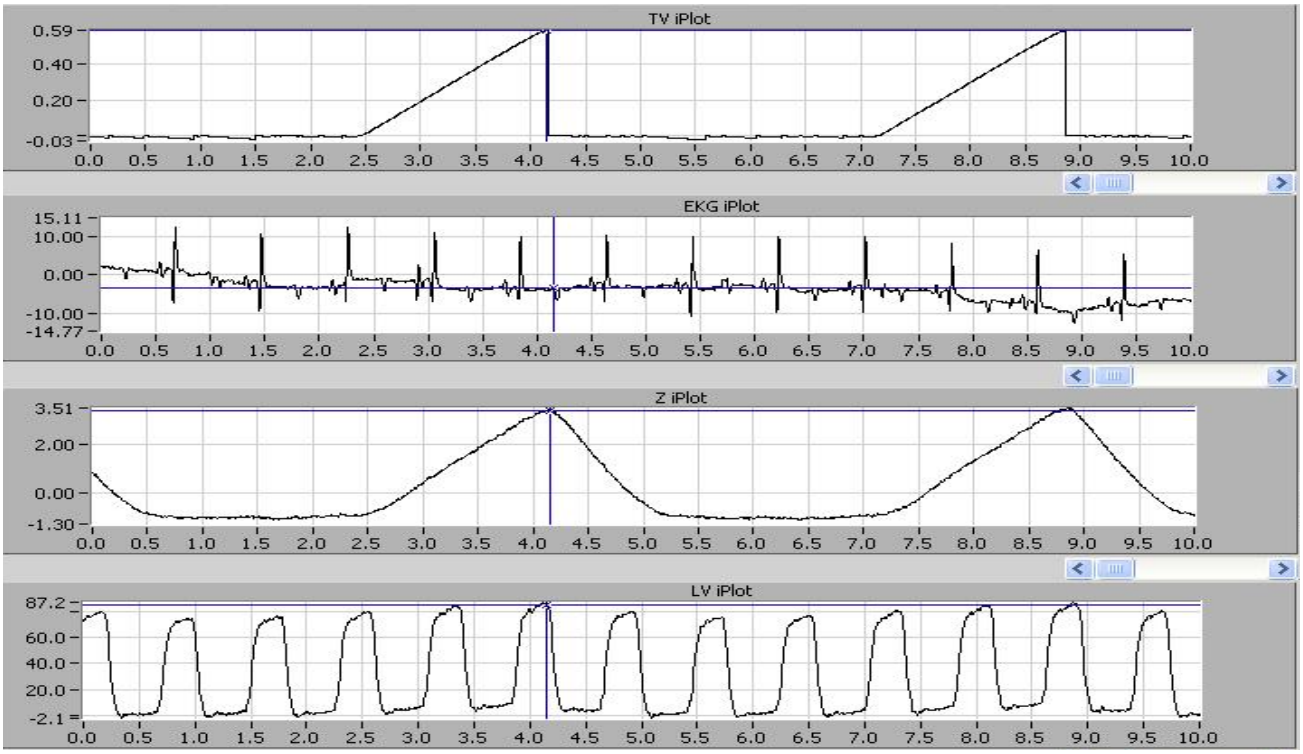

Figure 4: An example of the general overview window of the Labview program. This window was used to determine the general quality of the signals before analysis with the Labview program.

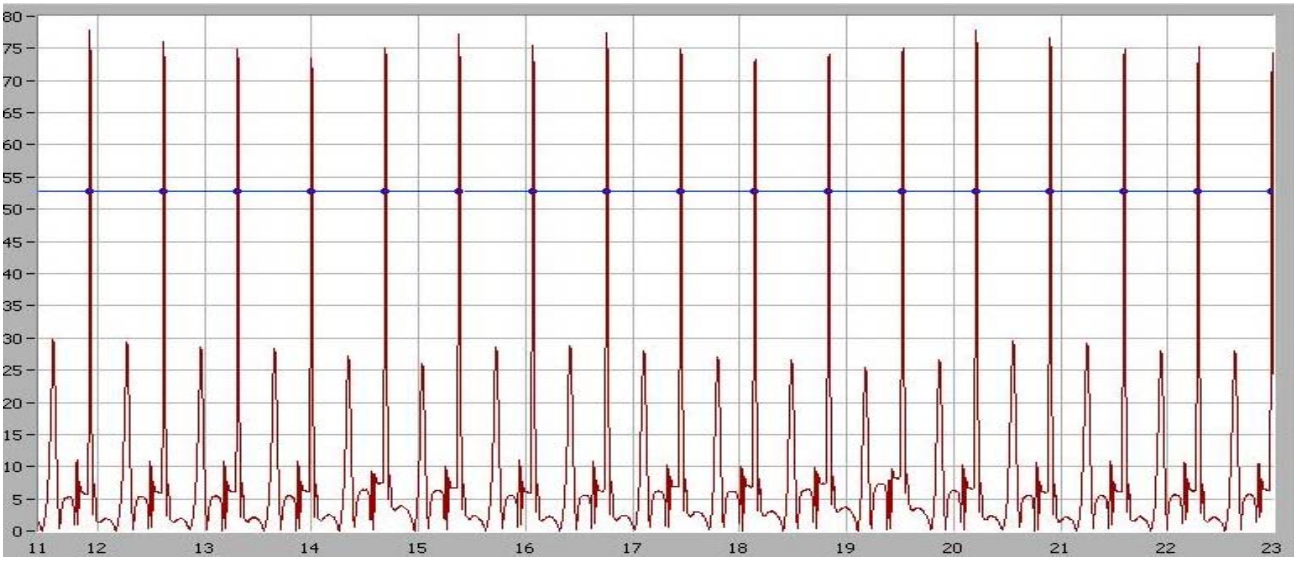

Figure 5: Showing the ECG run on the Labview program. The cursor was moved up or down until all R-waves had been detected as seen by the presence of dots where the linear cursor (horizontal line) meets the amplified R-waves (vertical lines).

The ECG count takes place by placing a horizontal linear curser on the R-wave. The program amplifies the R-wave and so allows the cursor to be selectively placed on it (so avoiding multiple counts per ECG cycle) as depicted in the figure above.

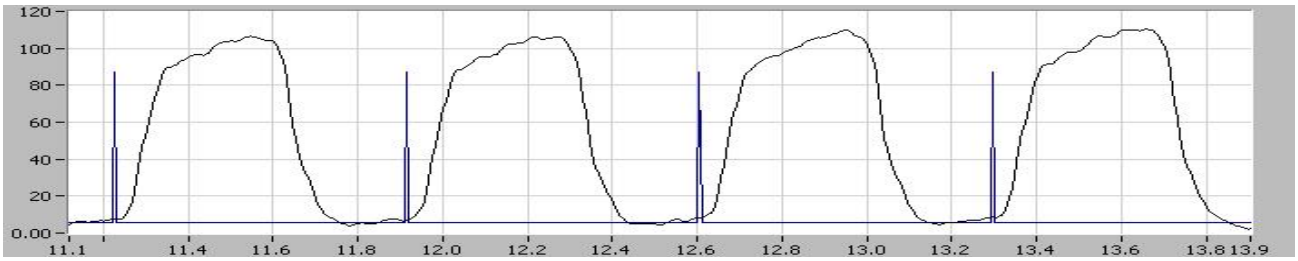

Figure 6

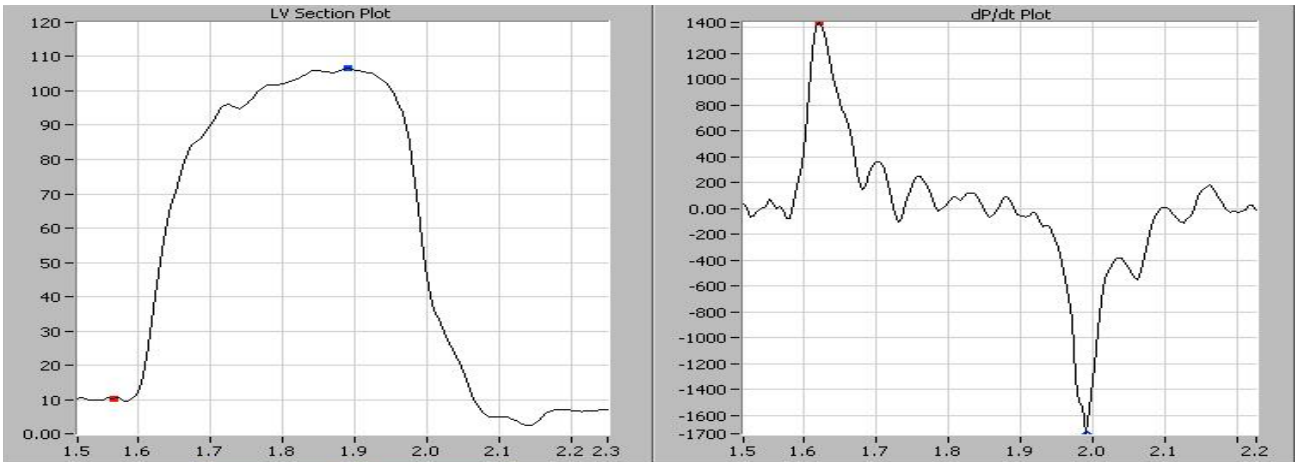

Figure 7

Figures 6 and 7: Depicting the LV run. Figure 6 showing the LVEDP measured by placing a cursor on it. Figure 7 shows the measurement of LVEDP, LVESP and dP/dT (automatically done by the program).

The left ventricular pressure was analyzed in two consecutive windows. The first window marked the beginning of the end diastole on the left ventricular pressure curves by placement of markers (figure 6). The second window measured the left ventricular end diastolic pressure (LVEDP), the peak of the left ventricular systolic pressure as well as the positive and negative dP/dt (figure 7).

The latter measurement happened automatically and involved accepting or occasionally rejecting the measurement if the signal was bad.

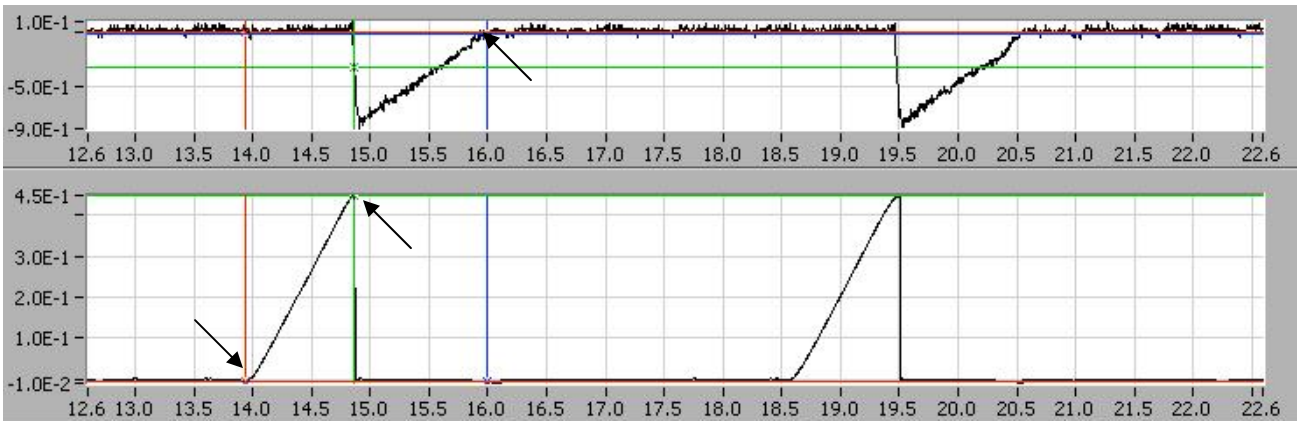

Figure 8: Showing the respiration run. The upper part of the window depicts the expiration channel and the lower one the inspiration. Arrows demonstrate cursors.

For the respiration signal, three cursors (shown above with arrows) were used to mark the beginning of inspiration, its peak and the end of expiration. From these measurements, the respiratory volumes were derived by the computer.

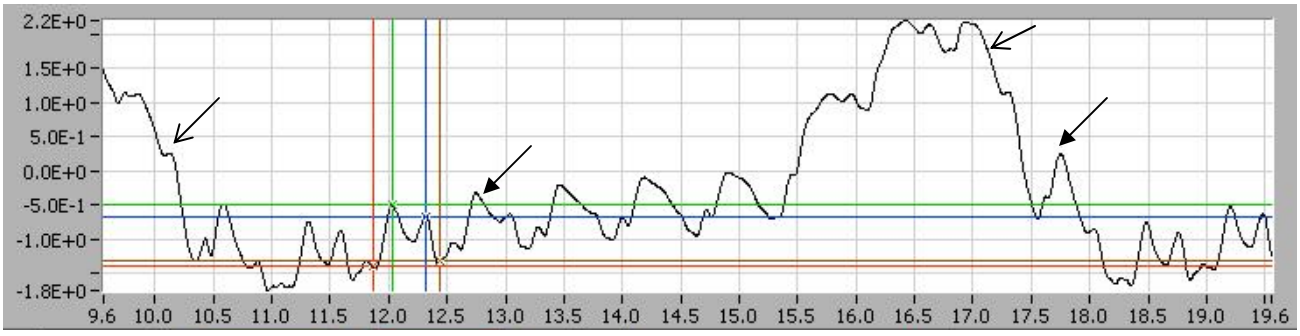

Figure 9: Showing the Z signals. Notice the larger respiratory derived Z signal (open arrows) on and between which the cardiac signals (filled arrows) are visible. The four parallel vertical lines are the cursors.

The respiratory and cardiac impedances were analyzed by using four cursors which measured the value and time of the signal at their placement points. One was placed at the beginning of the

respective Z signal; a second cursor was placed at the peak of the signal. If a second peak was available, a third cursor was placed on it, if not it was inactivated by mouse click on the inactivation icon in the window. The last cursor was placed at the end of the signal. From these measurements, the area under the Z curve, dZ and its peak were derivable.

The cardiac output value was automatically retrieved from the text files. After each run, the data was then stored as CUT files, retrievable as excel files.

3.9. Statistics

Correlation according to Merriam-Webstar´s Online Dictionary is defined as "a relation existing between phenomena or things or between mathematical or statistical variables which tend to vary, be associated, or occur together in a way not expected on the basis of chance alone".

Correlation statistics were performed with Pearson´s correlation coefficient, ``r´´. Pearson´s correlation coefficient measures the strength of the linear relationship between two variables e.g. ``X´´ and ``Y´´. It can take on the values from -1.0 to 1.0, where -1.0 = perfect inverse correlation, 0.0 = no correlation, and 1.0 = perfect positive correlation. r = 0 – 0.19 was regarded as very weak, 0.2 - 0.39 as weak, 0.4 – 0.59 as moderate, 0.6 – 0.79 as strong and 0.8 – 1 as very strong correlation (34). The coefficient of determination or r squared (R^2) can be interpreted as the proportion of variance in Y that is contained in X. Graphs were drawn using Microsoft Excel.

4. Results

The aim of this study was to determine if local subcutaneous bioelectrical impedance (bioimpedance, Z) correlates with respiration parameters (tidal volumes and respiration rates), fluid overload (fl) and cardiac output (CO); and could therefore serve as an indicator for changes in hemodynamic status. The experiments were carried out on eight female pigs (average weight 32.5±5 Kg). The results are based on data from six pigs because of an acquisition error on one pig leading to an unusable noisy signal and the premature death of a second one.

The pigs got subcutaneous electrode arrays (SubQ arrays) implanted on their left chests and pace-maker electrodes in their right atria, right ventricles and coronary sinuses. After 11.25±2.6 days, sufficient fibrous fixation of electrodes and arrays had occurred after which follow-up measurements were made. Verapamil and Metoprolol (6.8±1.8 mg each), saline and hydroxyethyl starch (HAES) were infused to create a fluid overload status. The variations in drug quantities result from variations in amounts needed to reduce stroke volume by 25% in individual animals.

4.1. Hemodynamic Parameters

4.1.1. Relationship Between Hemodynamic Parameters and Fluid Overload

Following the induction of heart failure, there was a decrease in continuous cardiac output (CO) and the mean arterial pressure (MAP), whereas the pulmonary capillary wedge pressure (PCWP), mean pulmonary arterial pressure (MPAP) and central venous pressure (CVP) increased (see subsequent figure). The CO decreased in litres/minute as follows: Mean of 3.2±0.2 at baseline, 2.7±0.2 at fluid overload 1 (fl1) and 2±0.1 at the fluid overload two (fl2). There was also a reduction of MAP 89.2 (baseline), 61.9 (fl1) and 54.6 (fl2) mmHg.

The MPAP increased from baseline, fl1 and fl2 respectively as follows: 13.4, 17.0 and 19.7. The CVP and PCWP had mean values of 2.3 and 2.8 at baseline, 6.6 and 7.4 at fl1; and 9.3 and 11.2 at fl2 respectively. All pressures are in mmHg.

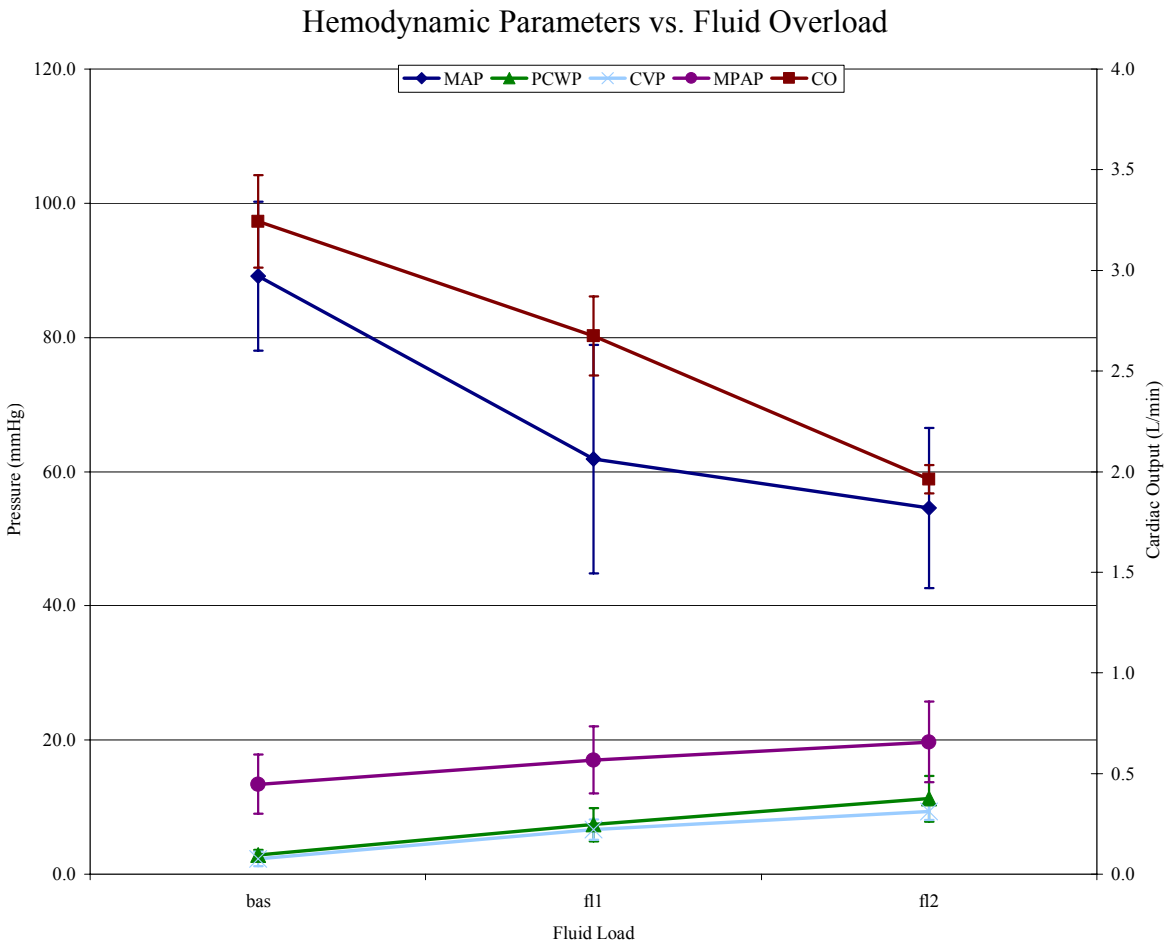

Figure 10: The relationship between MAP, CO, PCWP, MPAP and CVP over different fluid overloads. Whereas the CO and MAP diminished with increasing fluid overload, the PCWP, MPAP and CVP increased. bas, fl1 and fl2 stand for baseline, fluid overload 1 and fluid overload 2 respectively.

4.1.2. Relationship Between Heart Frequency and Fluid Overload

There was a decrease in heart frequency (HF) in all pigs between baseline and fl1. The HF averaged 90.7±11 at baseline and 77.1±14.6 at fl1. Between fl1 and fl2, there was a further decrease in HF to 73.4±16.2 at fl2 in five pigs and increase in one pig from 75 to 104 beats per minute.

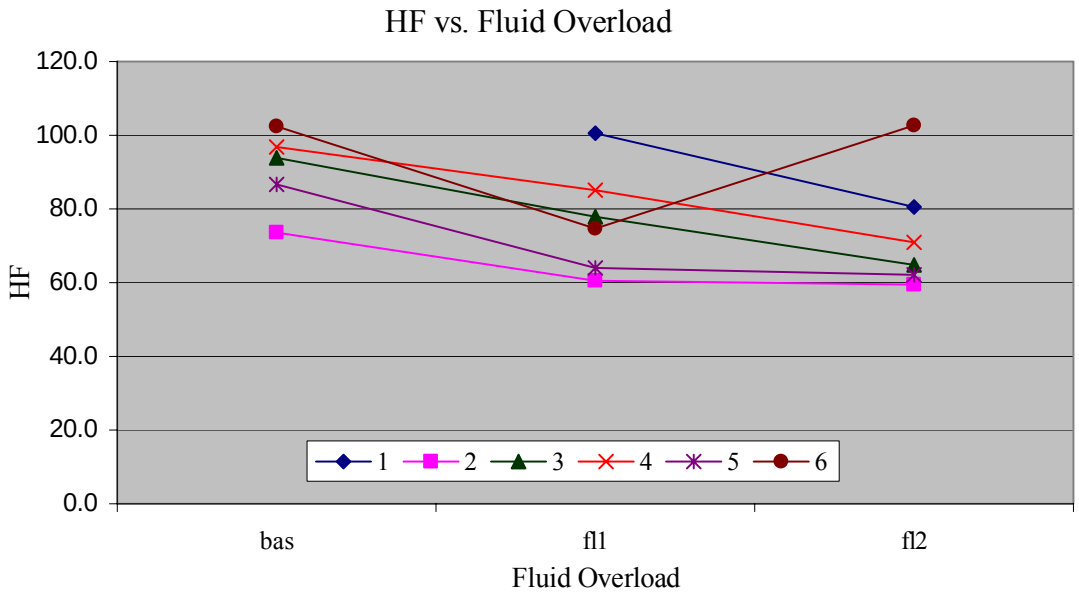

Figure 11: Relationship between heart frequency (HF) and fluid overload. Between baseline (bas) and the first fluid overload (fl1), HF decreased in all cases. Between fl1 and second fluid overload (fl2), HF decreased in all but one case.

4.1.3. Relationship Between LVEDP and Fluid Overload

All animals showed varying changes in left ventricular end diastolic pressure (LVEDP) between baseline and fl1 and between fl1 and fl2 after induction of heart failure. These changes seemed not consistent in one direction.

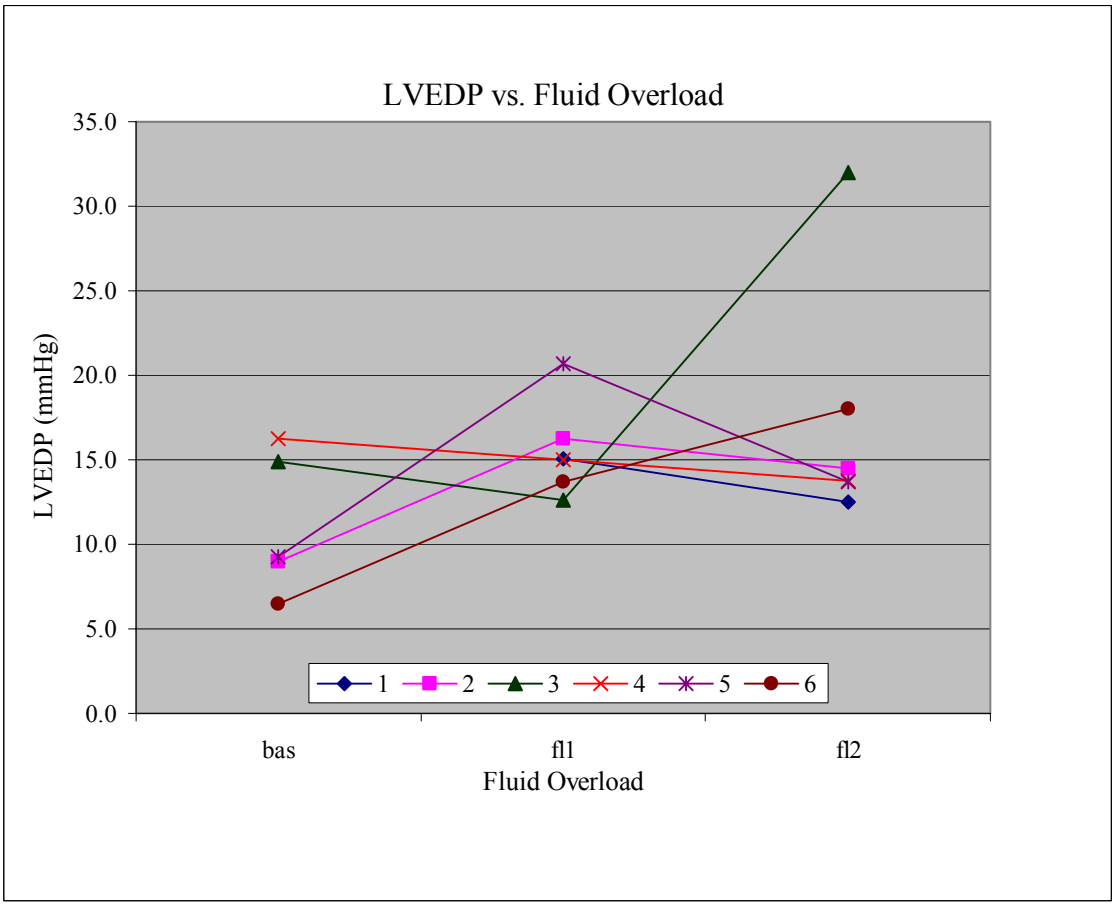

Figure 12: The relationship between left ventricular end diastolic pressure (LVEDP) and fluid load status (bas, fl1 and fl2) after heart failure induction. There seems to be no correlation.

4.1.4. Relationship Between CO and Fluid Overload

The continuous cardiac output (CO) decreased with an increase in fluid load status in all pigs at values between 3.7 and 3 in baseline to 2.8 and 2.3 in fluid load 1. Values in fluid load 2 were between 2.1 and 1.4. Measurements are in litres/minute.

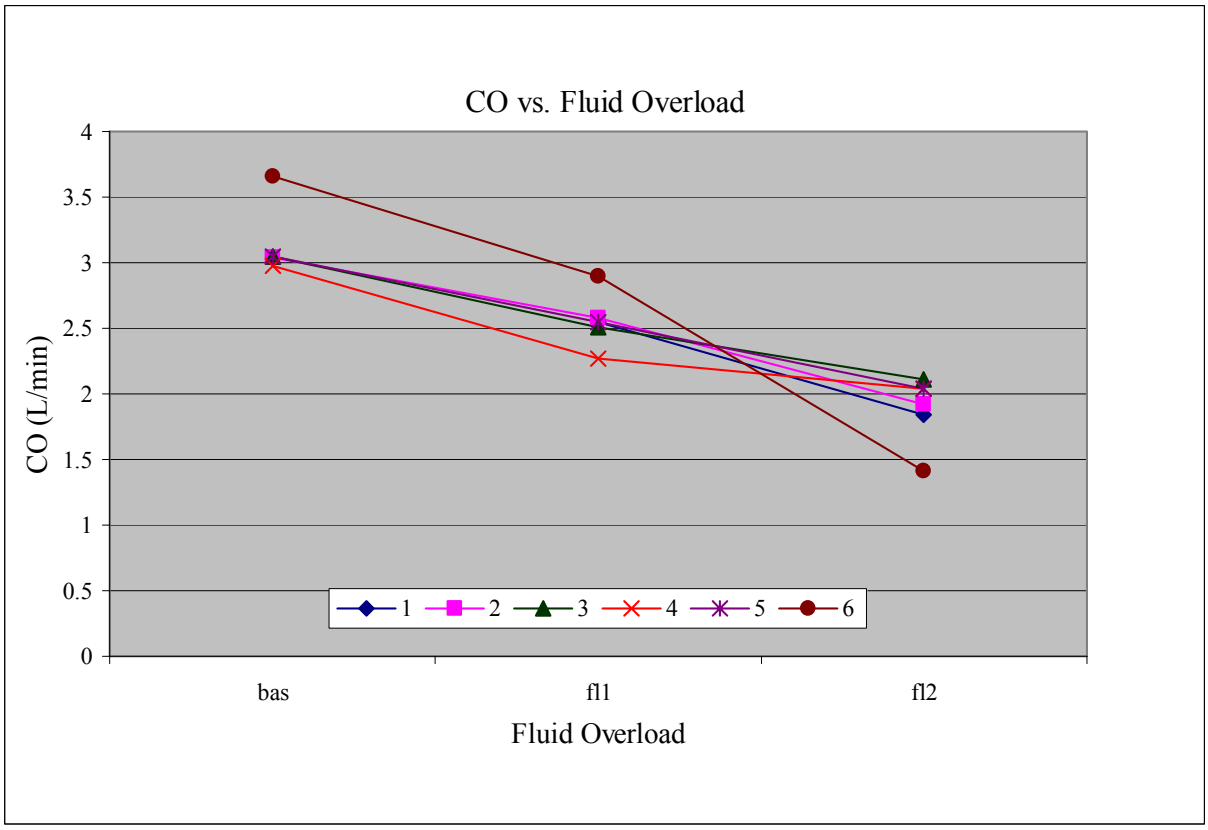

Figure 13: Showing relationship between cardiac output (CO) and fluid over load status (bas, fl1 and fl2).

4.1.5. Relationship Between CO and Percentage Change in Biompedance

There was a consistence in the relationship between cardiac output (CO) reduction and the percentage change in bioimpedance after induction of heart failure and fluid overload. The impedance dropped to 90.1% of its baseline value in fluid overload 1 (fl1) and then to 88.9% in fluid overload 2 (fl2) with R^2=0.8327. The corresponding CO dropped from 3.2±0.2 L/min to 2.7±0.2 L/min (84.4%) and 2.0±0.1 L/min (62.5%) in baseline, fl1 and fl2 respectively.

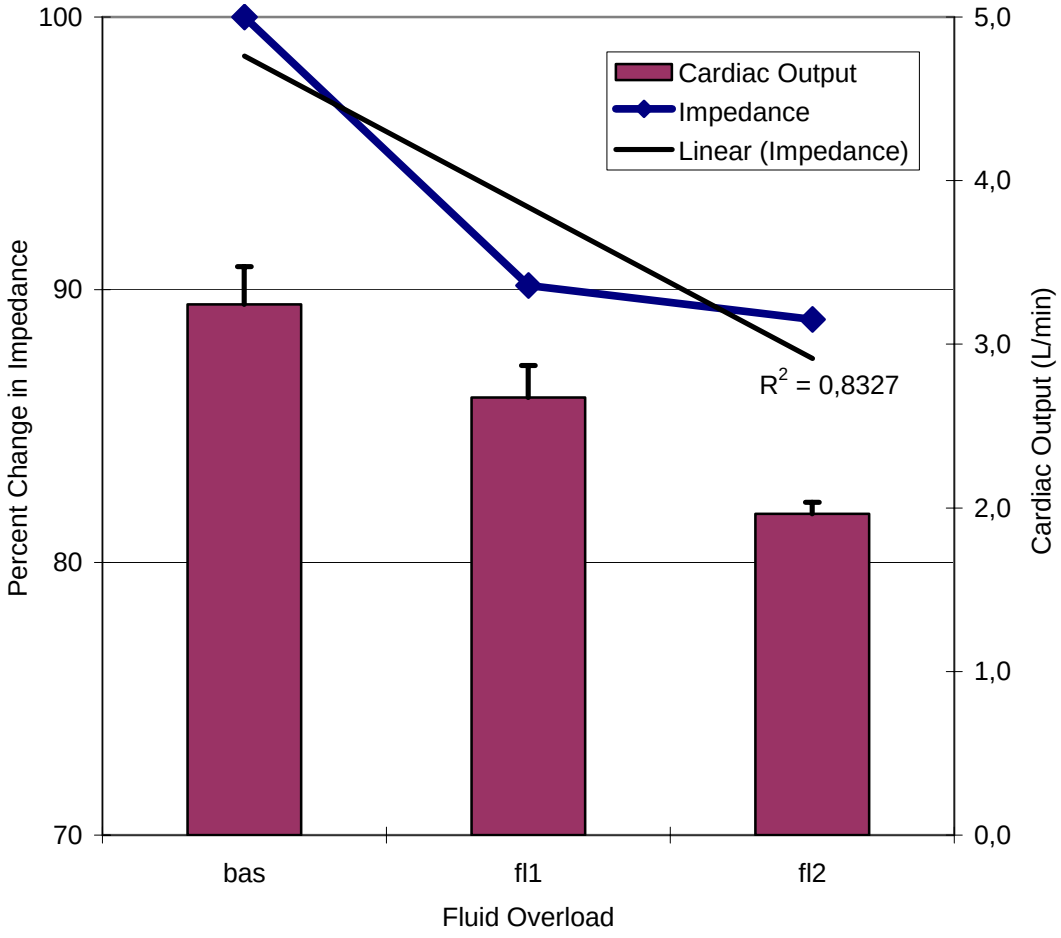

Figure 14: Showing the relationship between cardiac output (CO) reduction and the percentage change in impedance from baseline (bas), fluid overload 1 (fl1) and fluid overload 2 (fl2). The percentage change in impedance is depicted on the left vertical axis and shown as a line graph; and the corresponding CO on the right vertical axis shown as bar graphs.

4.2. Frequency Dependence of Bioimpedance

The magnitude of the bioimpedance signal varied greatly when recorded in different frequencies. Smaller frequencies generated larger amplitudes with 4 kHz, 12.5 kHz and 100 kHz generating relatively large, small and even smaller amplitudes, respectively.

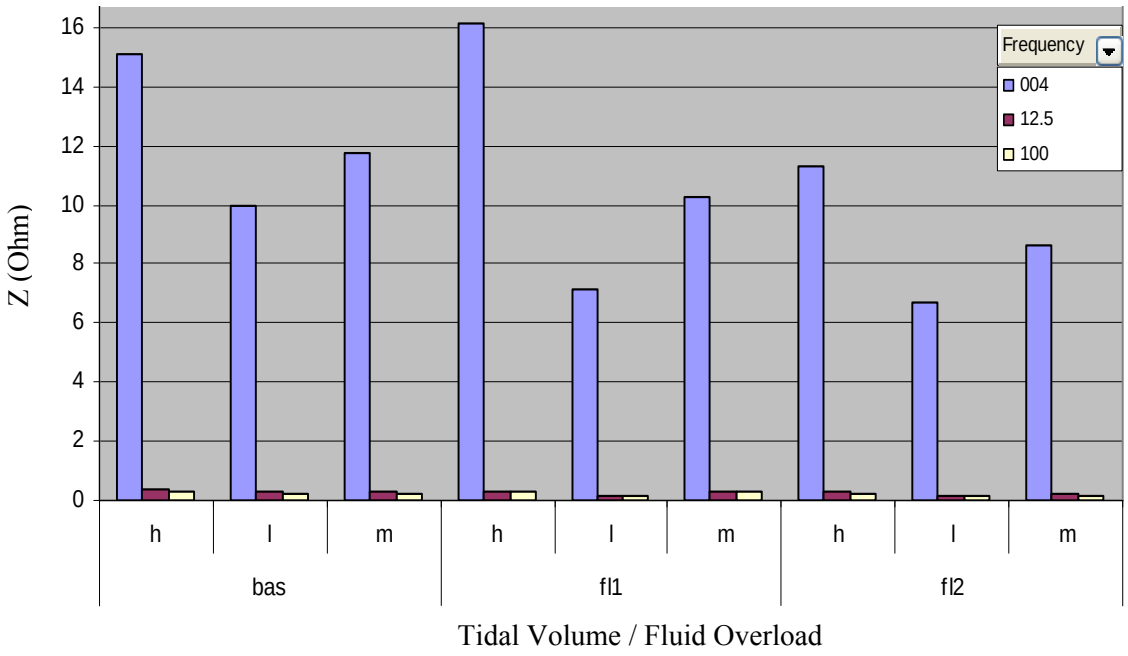

Figure 15: Depicting the frequency dependence of the magnitude of the impedance signal. The numbers on the legend represent the frequencies of 4, 12.5 and 100 kHz. Tidal volumes high, low and medium are represented as h, l and m, respectively.

4.3. Signal Entities

Different signal entities were derivable depending on the location of the measuring electrodes. The SubQ measurement showed an almost purely respiration-derived impedance signal with occasional cardiac components. The intra-cardiac to SubQ array measurements showed a respiratory impedance signal superimposed by the smaller higher frequency cardiac impedance signals. The signals recorded between the right ventricle and SubQ had more pronounced cardiac features than the one recorded between RV, CS and SubQ. In the intra-cardiac configuration, only the cardiac signal was clearly evident and the respiratory signal could only be made visible after low pass filtering (for exact location of intracardiac electrodes, see section 3.6.3).

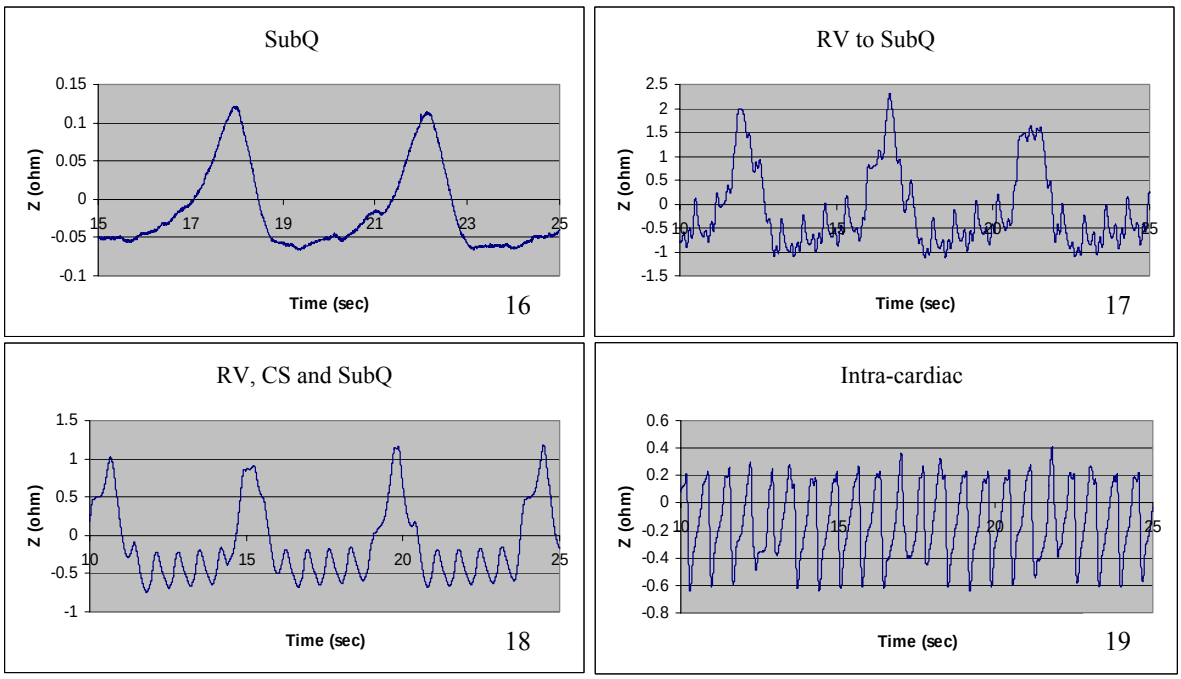

Figures 16 - 19: Showing the different signal entities resulting from placement of electrodes in different positions. 16) All electrodes from the SubQ array. 17) Two electrodes in the SubQ array and two in the right ventricle (RV). 18) Two electrodes in the SubQ array, one in the RV and one in the CS. 19) All electrodes intra-coronary.

4.4. Absolute Bioimpedance Measurement (PSA)

4.4.1. Relationship Between Absolute Bioimpedance, CO and Fluid Overload Status

The absolute bioimpedance decreased in nine of ten measurements with a decrease in cardiac output (CO) and increasing fluid overload (fl) status. The average absolute Z of the pigs declined from a mean of 439.5 Ohm in baseline, to 420.1 in fl1 and 403.9 in fl2. The figure below shows the absolute Z of individual pigs relative to the average cardiac output. The pigs showed a decrease in Z with an increase in fluid load. Pig 6 showed an increase from baseline to fl1 and then a decrease from fl1 to fl2. Pig 1 showed minimal changes in Z.

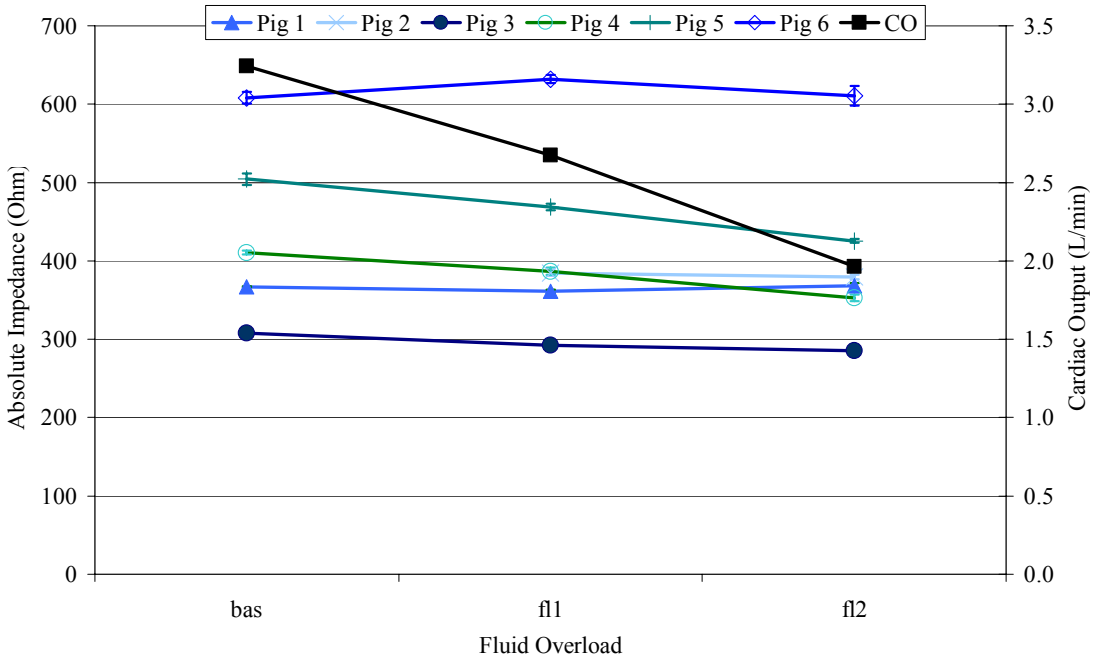

Figure 20: Showing on the Y-axis absolute impedance on the left and cardiac output (labelled CO) on right over the three fluid over load levels (baseline, fl1 and fl2).

4.4.2. Relationship Between Mean Absolute Bioimpedance, CO and Fluid Overload Status

The mean absolute bioimpedance (Z) declined from 100%, to 95.8% and 92.2% (R^2=0.989). The corresponding CO was 100%, 82.4% and 60.5% at baseline, fl1 and fl2, respectively.

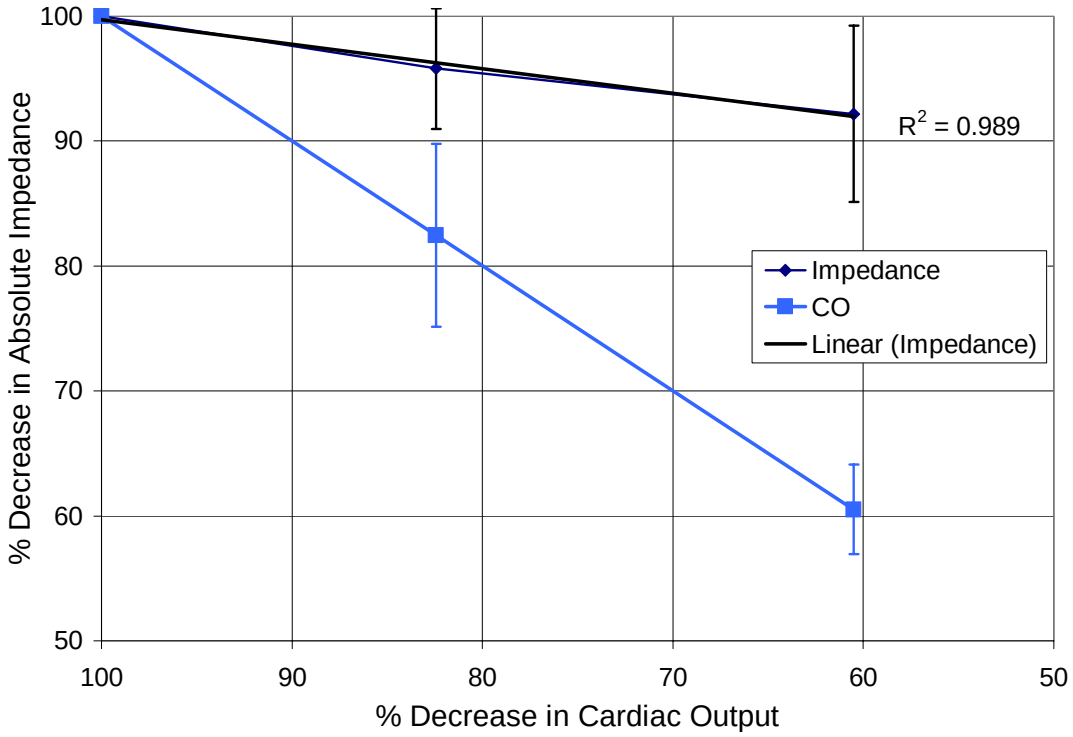

Figure 21: Showing the percentage change in impedance (Z) and the corresponding percentage change in cardiac output (CO) over bas, fl1 and fl2.

4.5. Pulmonary Bioimpedance

4.5.1. Temporal Relationship of Bioimpedance and Respiration

The temporal relationship of the bioimpedance and respiratory curves was such that their beginnings, peaks and ends coincided. Spontaneous breaths too had impedance correlates.

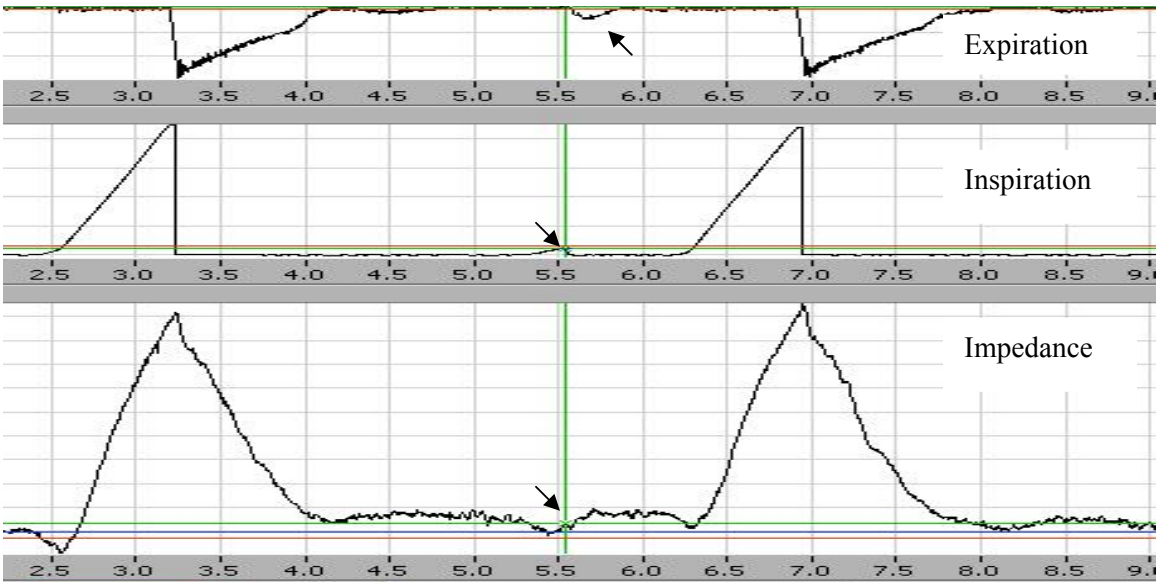

Figure 22: Showing the temporal relationship between inspiration, expiration and the pulmonary respiratory Z. Note the spontaneous breath signal and its correlate (arrowed). Inspiration and expiration are recorded on two different channels.

4.5.2. Relationship of Bioimpedance and Respiratory Rates

There was a very strong correlation between the rate of respiration-derived bioelectrical impedance and the respiratory rate. This was noticeable at bas, fl1 and fl2 (R^2=0.99).

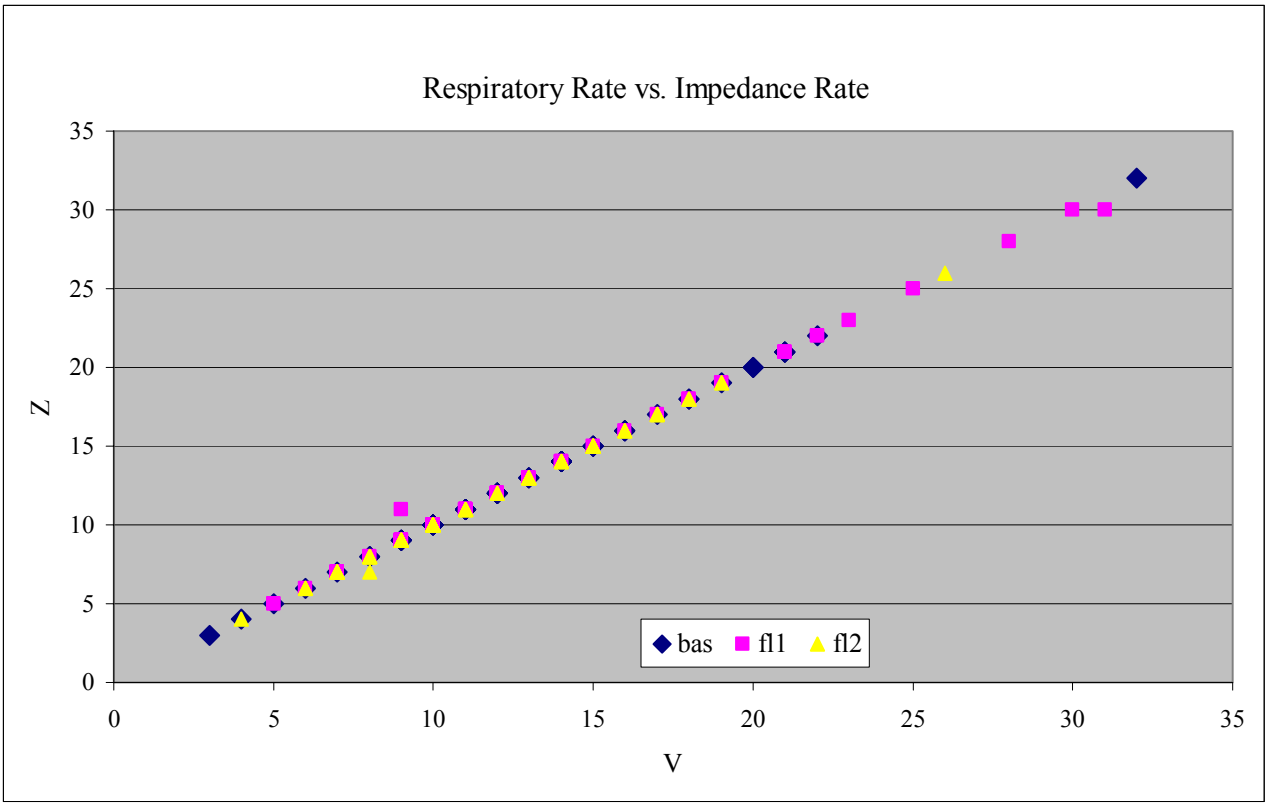

Figure 23: Showing the high correlation between respiration rate (V) and respiration-derived impedance rate (Z) in baseline, fluid overload 1 (fl1) and fluid overload 2 (fl2).

4.5.3. Relationship Between Bioimpedance and Fluid Overload

There was no clear relationship between change in ventilation-derived respiration bioelectrical impedance (RVZ delta) and fluid overload (fl). There was no consistency in the relationship either in individual pigs or in all pigs collectively.

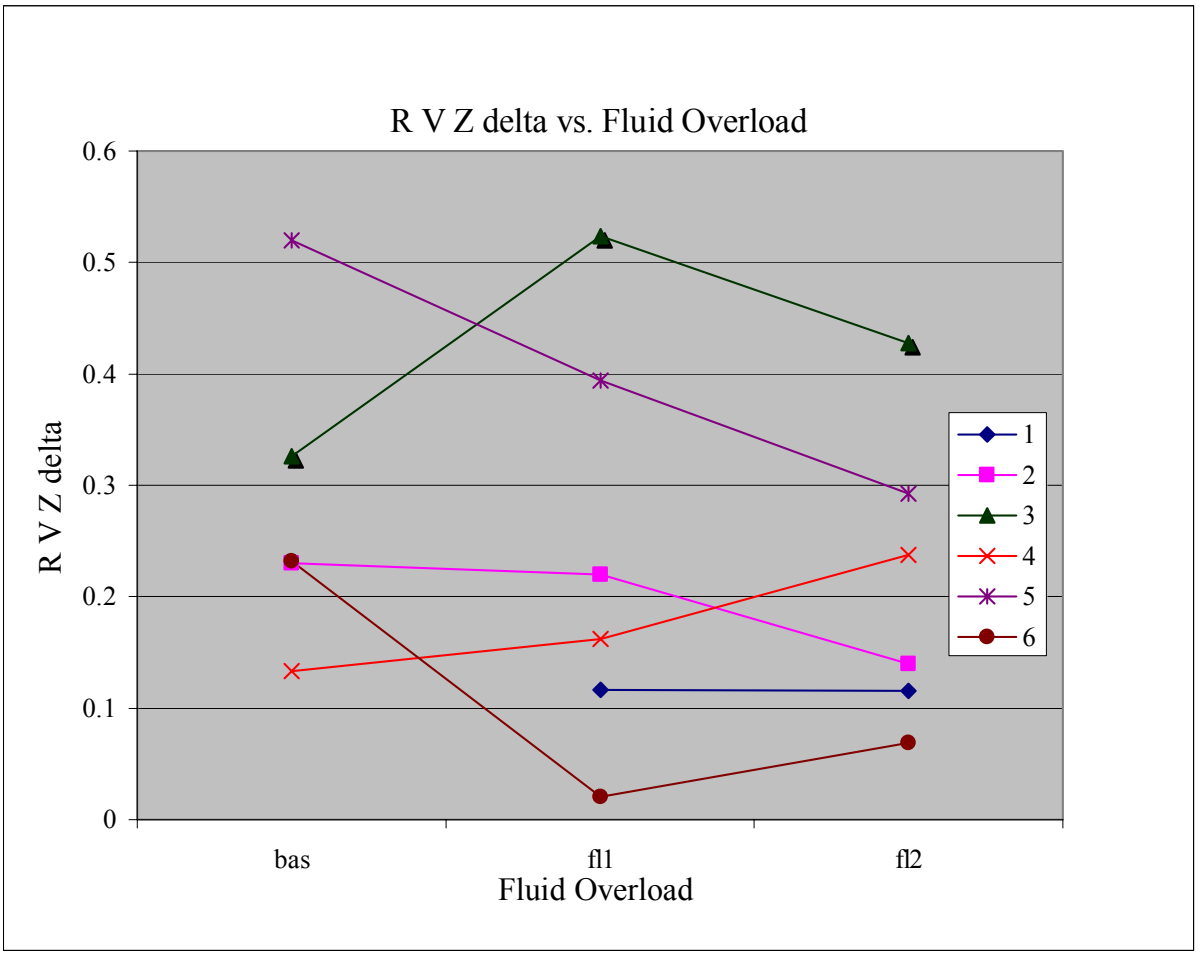

Figure 24: Showing the trends of individual ventilation-derived respiratory impedance (RVZ). The numbers in the legend show pig numbers.

4.5.4. Relationship Between Bioimpedance (Area Under Curve) and Fluid Overload

Three of five pigs showed a decrease in area under respiratory bioelectrical impedance curve (RVZ area) between baseline and fl1. Five out of six showed a decrease between fl1 and fl2.

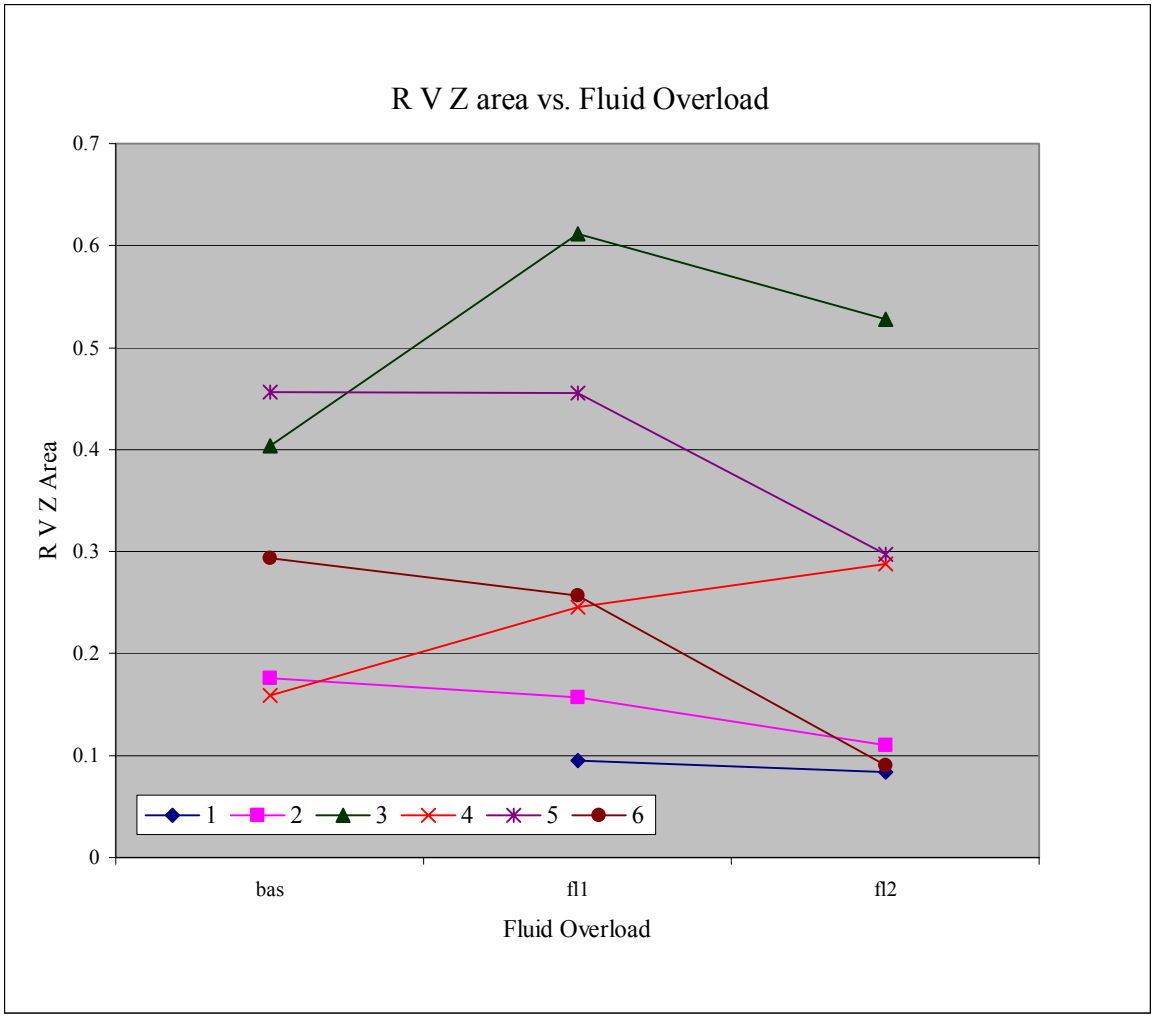

Figure 25: Showing the trends of area under the individual pigs' ventilation-derived respiratory impedance (RVZ). The numbers in the legend show pig numbers.

4.5.5. Relationship Between Bioimpedance and Tidal Volume

The high tidal volume (TV), medium TV and low TV all resulted in corresponding magnitudes on the bioelectrical impedance signal. Congestion resulted in a decrease in magnitude of Z, hence a continuous decrease in Z from baseline, fl1 and fl2 (described in section 4.1.5).

In low to medium TV, all pigs showed an increase in Z with an increase in tidal volume except one pig whose Z fell from 0.15 to 0.13 ohms. There was an increase in Z with tidal volume in all pigs between medium TV and high TV. The mean Z in low TV was 0.27±0.12 ohms, in medium TV 0.29±0.15 ohms and in high TV 0.4±0.21 ohms. The overall mean Z was 0.32±0.16 ohms in baseline, 0.26±0.17 ohms in fluid overload 1 and 0.22±0.14 ohms in fluid over load 2.

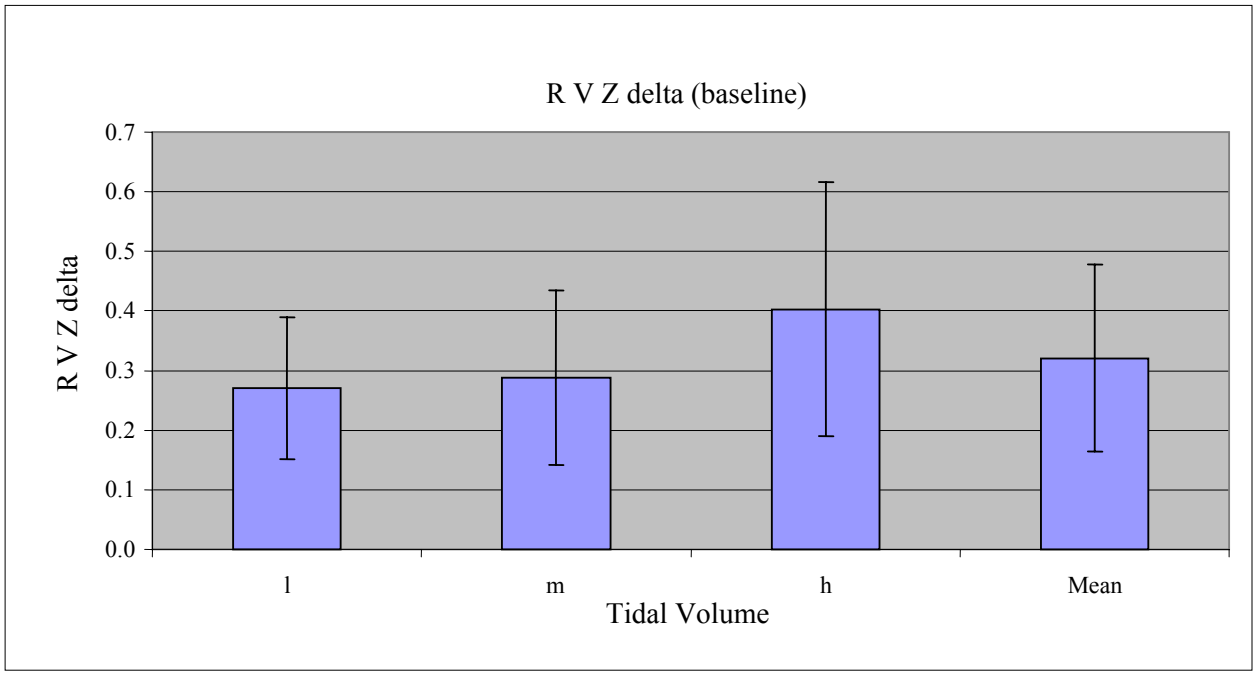

Figure 26: Showing the relationship between RVZ delta and tidal volume. l, m and h stand for low, medium and high tidal volumes, respectively.

At fl1 between low and medium tidal volume (TV), all pigs except one showed an increase in delta Z with an increase in TV. The Z of the one pig fell from 0.2 to 0.16 ohms. Between medium and high TV, all pigs showed an increase in Z with an increase in TV except one pig whose Z fell from 0.2 to 0.1 ohms. The mean Z in low TV was 0.18±0.1 ohms, in medium TV 0.27±0.16 ohms and in high TV 0.32±0.2 ohms. The overall mean Z was 0.26±0.17 ohms.

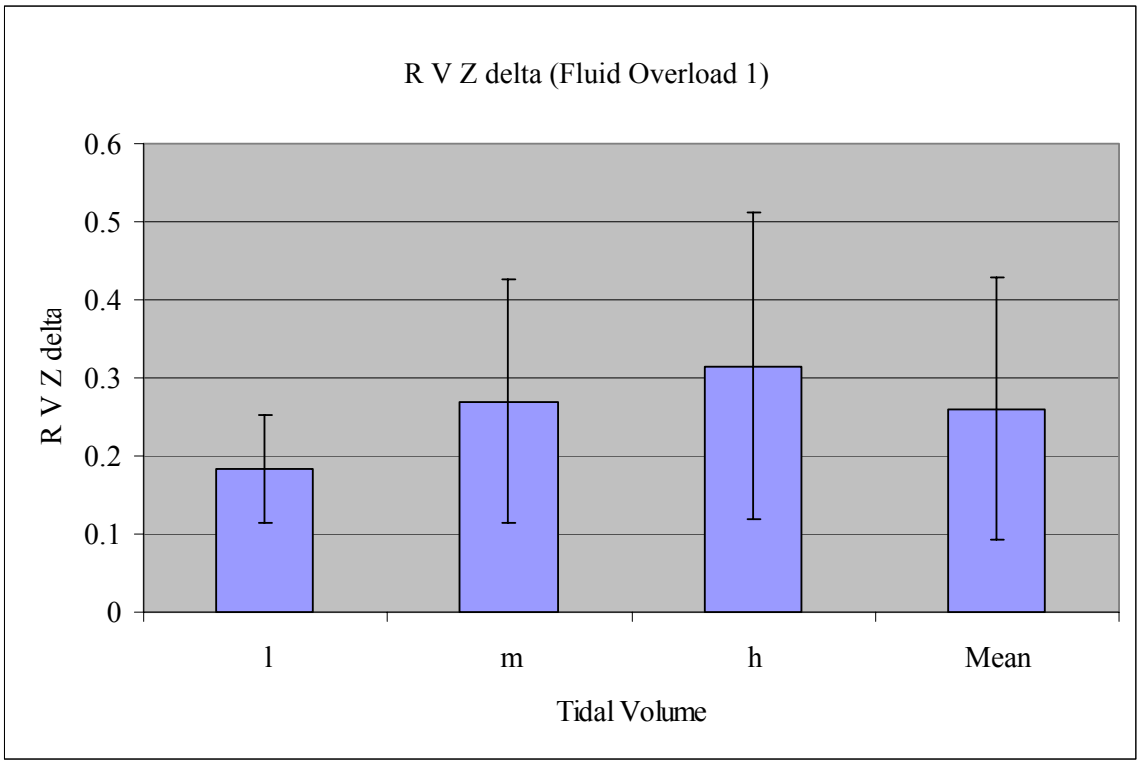

Figure 27: Showing the relationship between RVZ delta and tidal volume (TV) in fl1. l, m and h stand for low, medium and high tidal volumes, respectively.

In fl2, there was a corresponding increase in Z with an increase in tidal volume between low, medium and high tidal volumes. The mean increase in Z was 0.18±0.12 ohms in low TV, 0.21±0.14 ohms in medium TV and 0.26±0.17 ohms in high TV. The overall mean was 0.22±0.14 ohms.

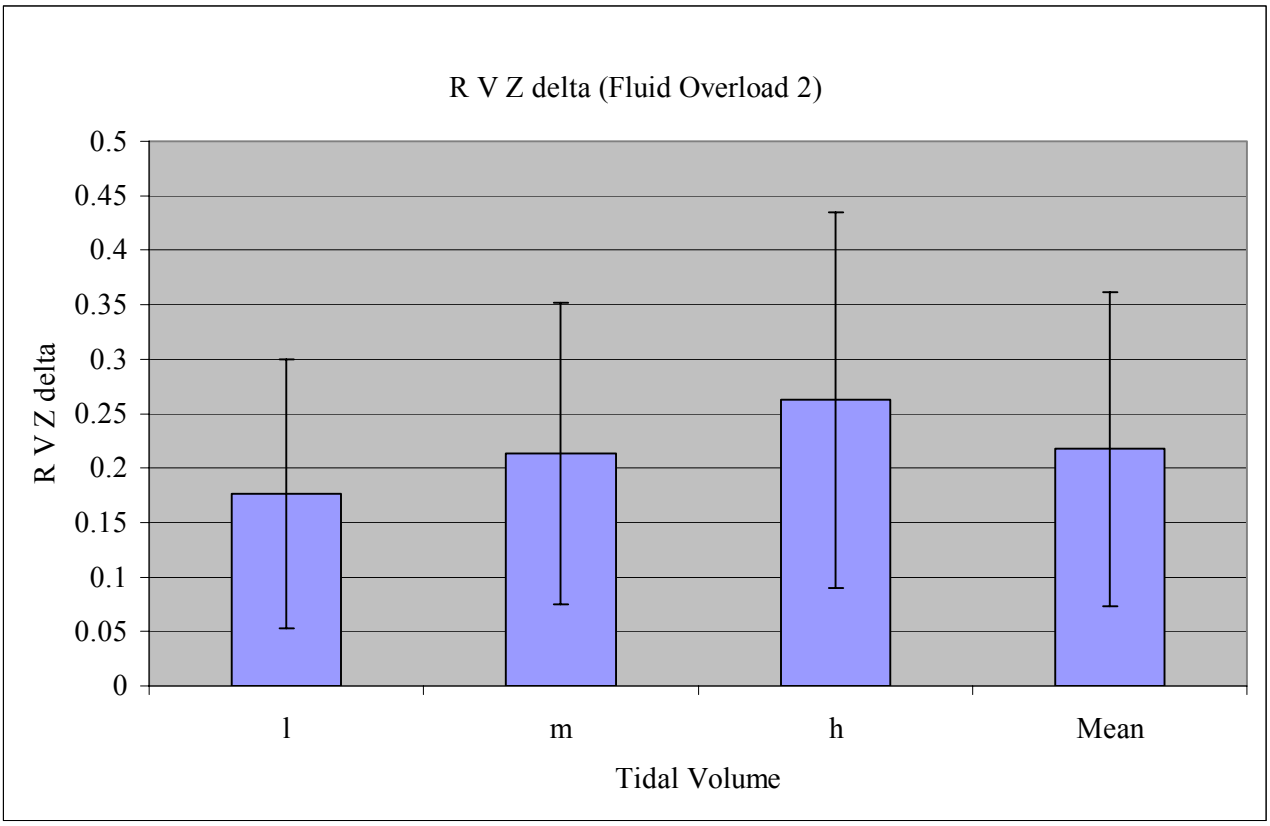

Figure 28: Showing the relationship between change in ventilation-derived impedance (RVZ delta) and tidal volume in fl2. l, m and h stand for low, medium and high tidal volumes, respectively.

4.6. Cardiac Bioimpedance Results

4.6.1. Temporal Relationship Between Intra-cardiac Bioimpedance, ECG and LV Pressure

The intra-cardiac impedance signal had two peaks; one corresponding with the P-wave and the second one to the QRS-complex of the ECG wave. Between the peaks was a small depression. The minimum impedance wave value was corresponding with the T-wave of the ECG.

The maxima of the impedance signals corresponded with low left ventricular pressures and the minima with the high ones. Its relationship with LVEDP was somewhat similar to the usual LVEDP and volume wave.

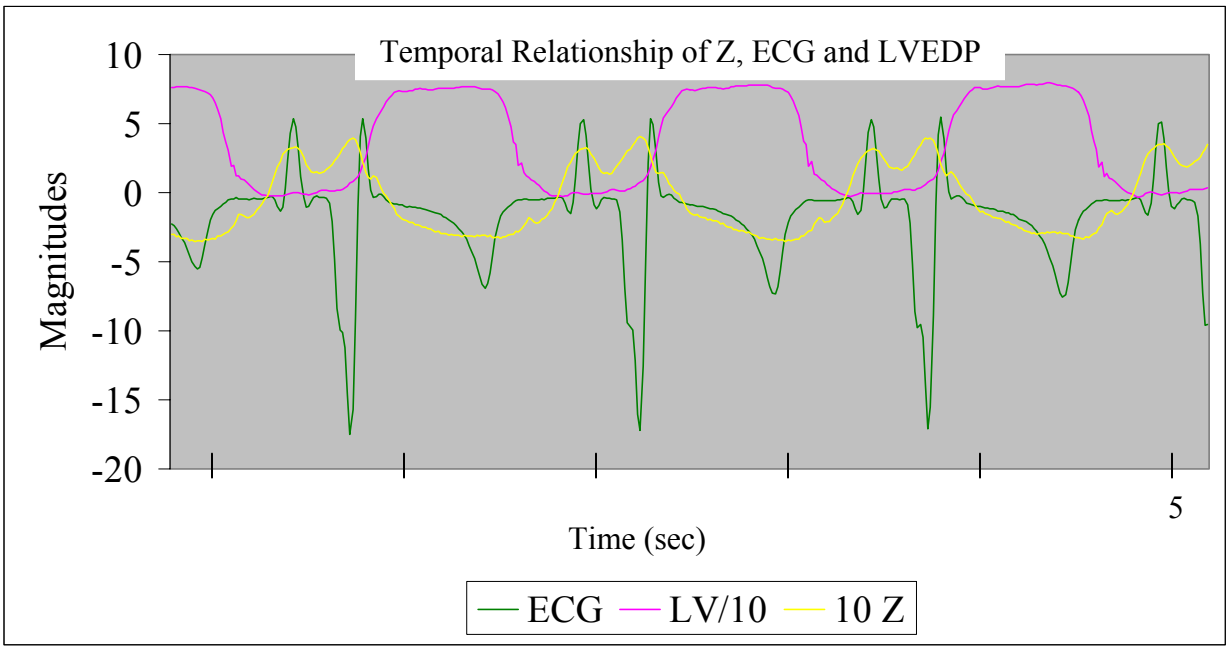

Figure 29: Showing 10Z, ECG and LVEDP/10 on one temporal scale (vertical scales modified for presentation). ECG is electrocardiograph, Z is impedance and LV is left ventricular pressure.

4.6.2. Relationship Between Intra-cardiac Bioimpedance Rate and Heart Rate

The number of ECG signals and the Z signals showed a very strong correlation (R2=0.94). As evident in preceding figure, every Z signal has a corresponding ECG signal. The Labview program could not recognize some P-waves, and either double counted or missed some. This resulted in a miscount of ECG signals leading to some miscorrelation.

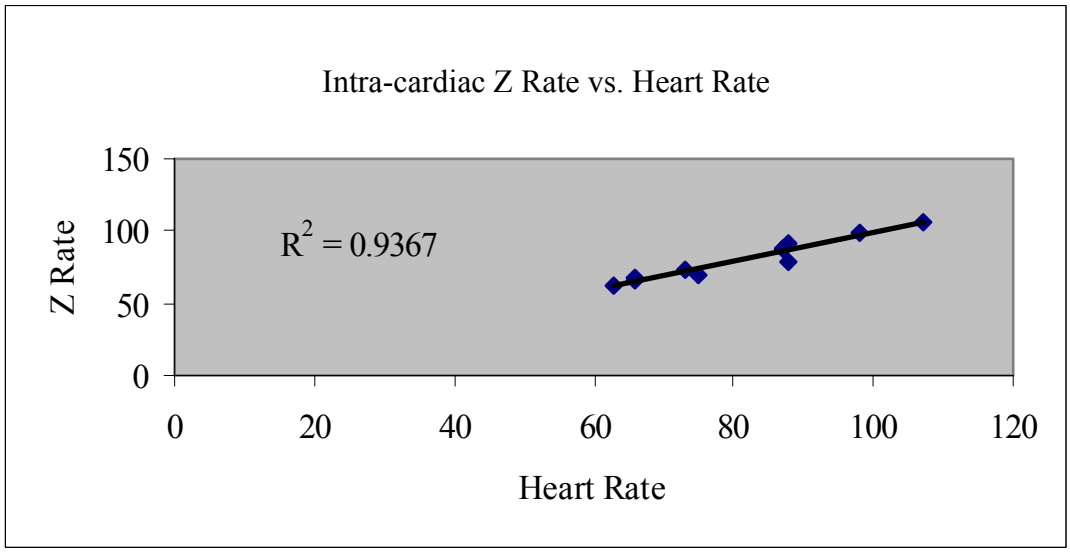

Figure 30: The heart rate and the intra-cardiac impedance signals (Z) rate showed a high correlation R^2=0.94.

4.6.3. Effect of Respiration on Intra-cardiac Bioimpedance

The effect of respiration on intra-cardiac Z can also be made visible without filtering. In this case, the Z follows the rhythm of the ECG but its magnitude is increased by inspiration and decreased by expiration to the original value.

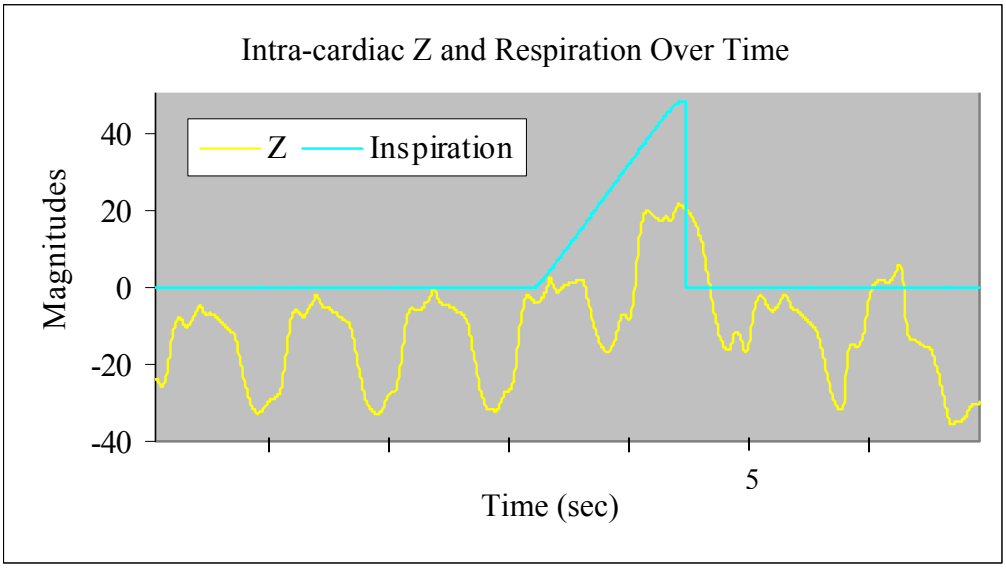

Figure 31: Showing the effect of respiration on intra-cardiac Z. The average value of the Z signal increases during inspiration and decreases during expiration.

4.6.4. Relationship Between LVEDP and Area Under the Intra-cardiac Bioimpedance

There was generally a weak correlation between LVEDP and the area under the intra-cardiac bioimpedance signal (R^2 between 0.0003-0.58 in individual pigs, see subsequent figures). This is true for individual pigs and for all pigs collectively.

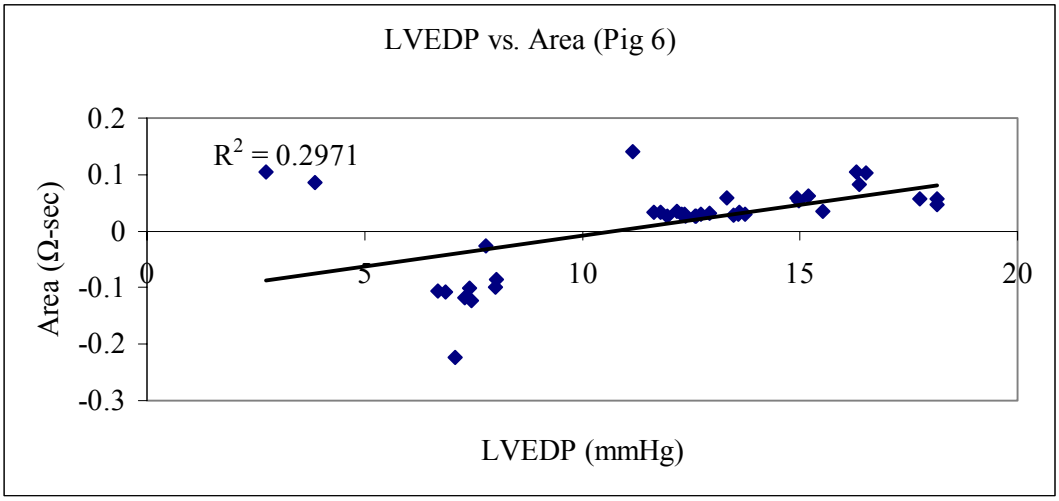

Figure 32

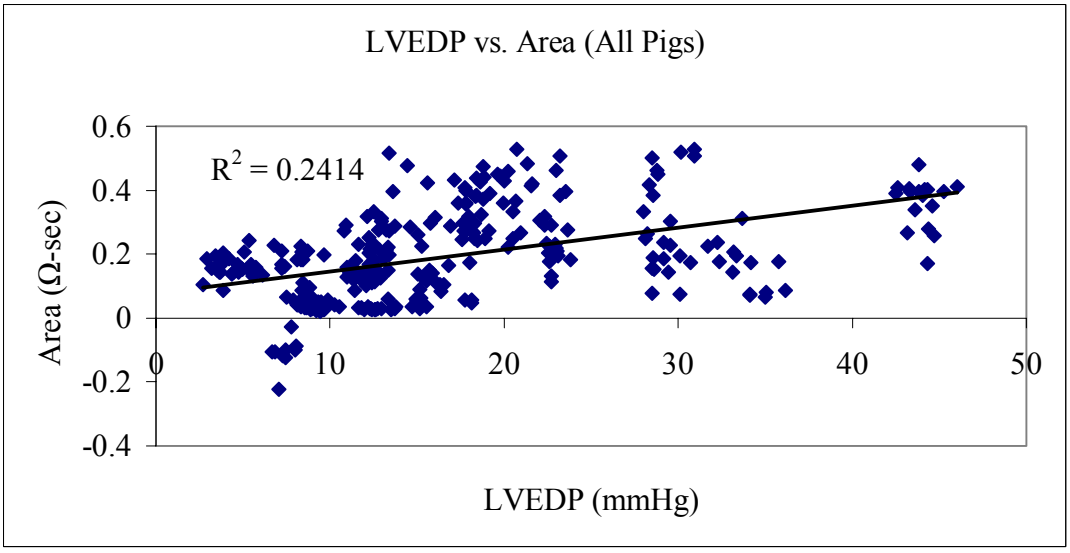

Figure 33

Figures 32 and 33: Showing weak correlation between LVEDP and areas under curve of intra-cardiac Z signal. Figures 32 and 33 show results from an individual pig and from all pigs, respectively.

4.6.5. Relationship Between Intra-cardiac Bioimpedance and LV Pressure Difference

The stroke Z was calculated as the difference between the left ventricular end systolic impedance and the left ventricular end diastolic impedance (ZS-ZD). This was then plotted against the difference between the left ventricular end systolic and end diastolic pressures (PS-PD). A strong correlation between the two was noticeable (R^2=0.6). This was true for individual pigs but was not evident when all pigs were plotted together, thus highlighting the individual differences between pigs. When all pigs were plotted together on one graph, the data from individual pigs are visible as clusters.

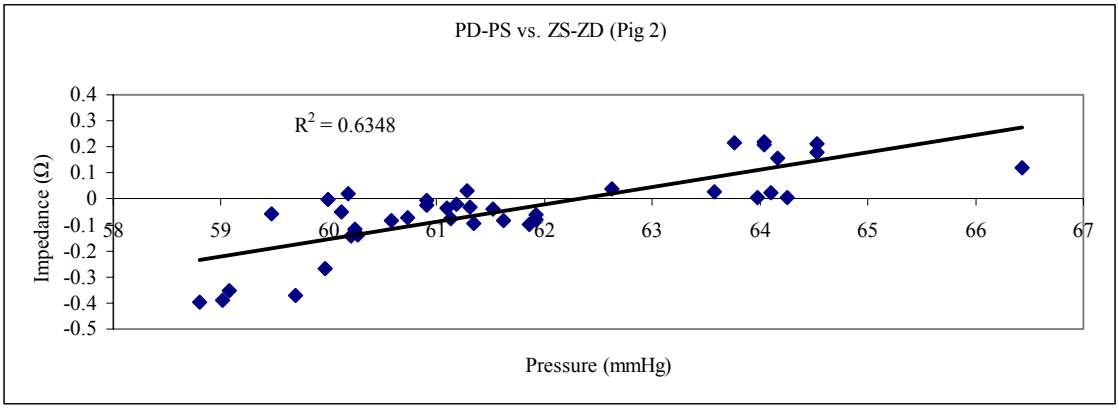

Figure 34

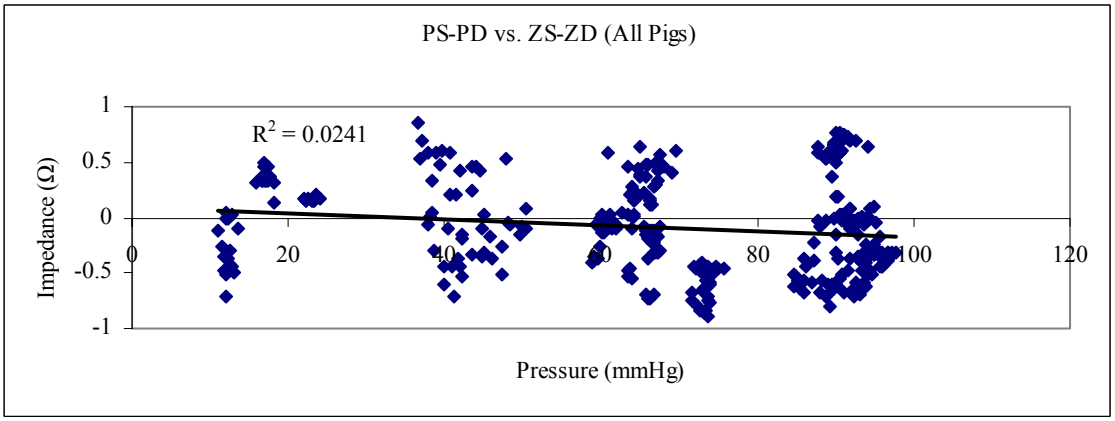

Figure 35

Figures 34 and 35: Showing relationship between change in pressure between systole and diastole (PS-PD) and the corresponding change in intra-cardiac impedance (ZS-ZD). Figures 34 and 35 show results from an individual pig and from all pigs, respectively.

4.6.6. Relationship Between Intra-cardiac Bioimpedance (Area Under Curve) and LV Pressure Difference

The end systolic and end diastolic pressure difference was also calculated and plotted against the area under the intra-cardiac Z curve. The results showed a minimal correlation between the two. The area under the intra-cardiac Z curve was independent of the pressure differences.

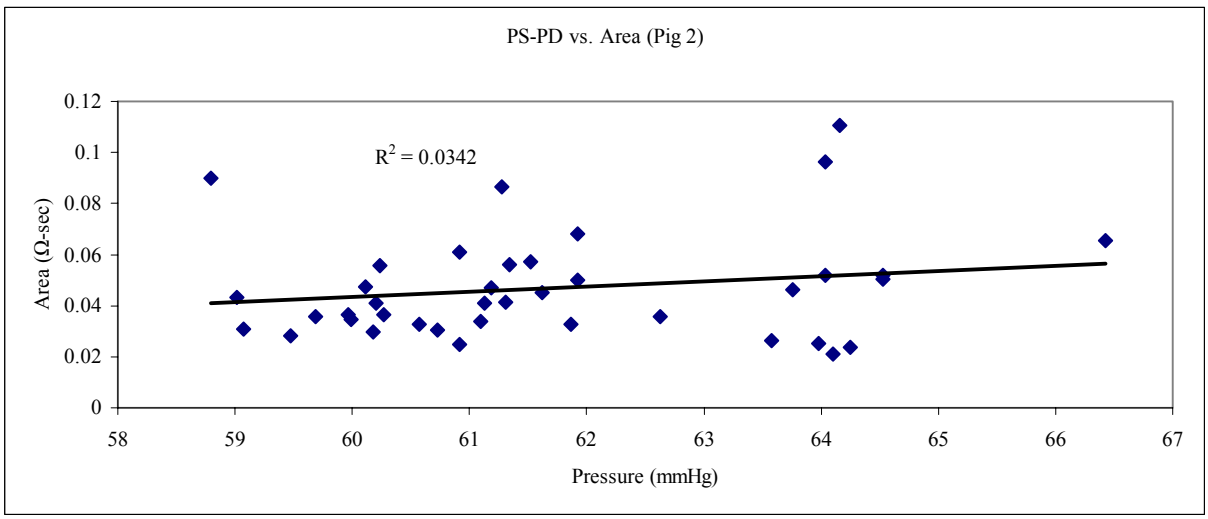

Figure 36

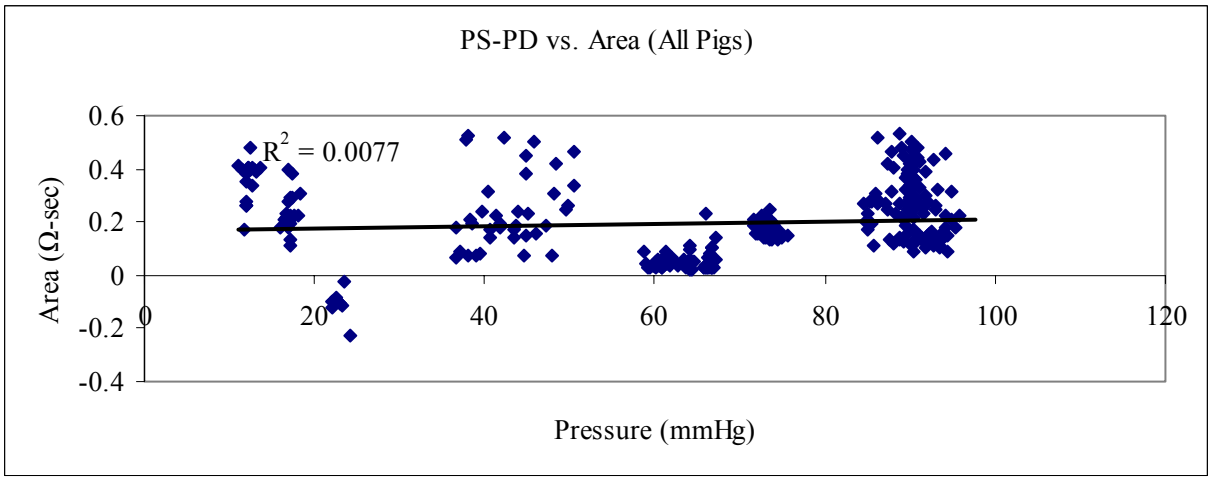

Figure 37

Figures 36 and 37: Showing the poor correlation between change in pressure between systole and diastole (PS-PD) and the corresponding change in area under the intra-cardiac Z curve. Figure 36 shows results from an individual pig and 37 of all pigs.

4.6.7. Relationship Between Intra-cardiac Bioimpedance (Peak Value) and LV Pressure Difference

A plot of the calculated difference in systolic and diastolic pressure (PS-PD) against the maximum deflection (peak) of the impedance signal showed differing correlations in individual pigs (R^2= between 0.2 and 0.9) and a very weak correlation when all pigs are taken collectively.

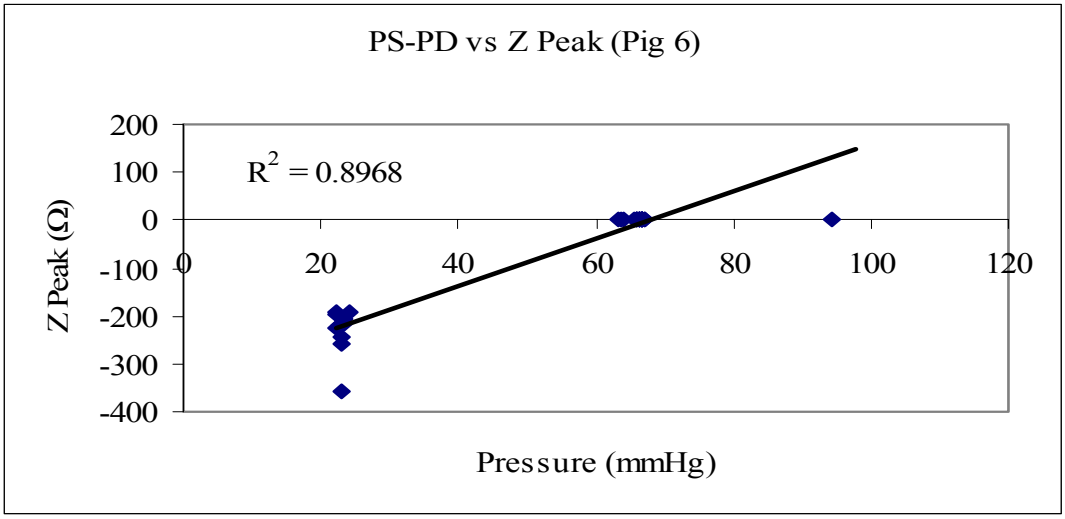

Figure 38

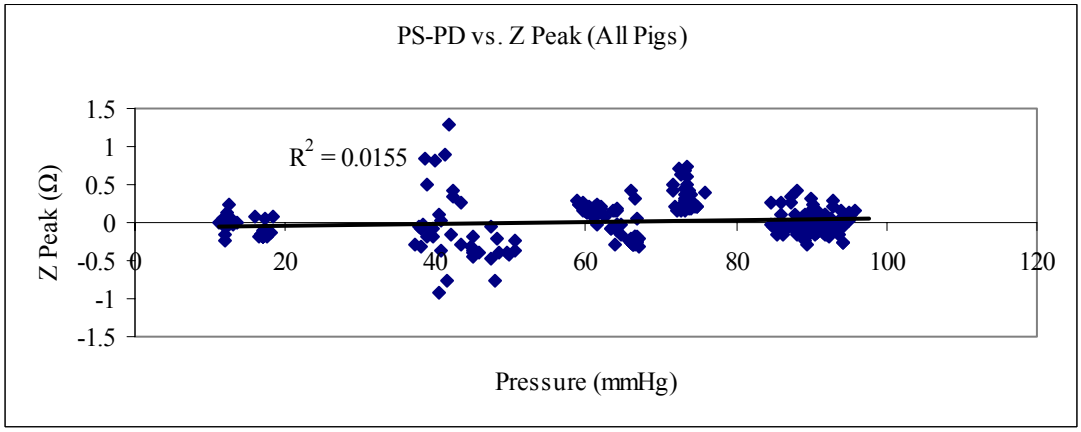

Figure 39:

Figures 38 and 39: Showing the relationship between change in pressure between systole and diastole (PS-PD) and the maximal deflection in Z. There was no correlation (R^2=0.0155). Figure 38 shows results from an individual pig and 39 of all pigs.

4.6.8. Relationship Between Intra-cardiac Bioimpedance (Area Under Curve) and LV Pressure

The LVEDP showed moderate correlations with the area under the Z curve both in individual pigs and in all pigs collectively.

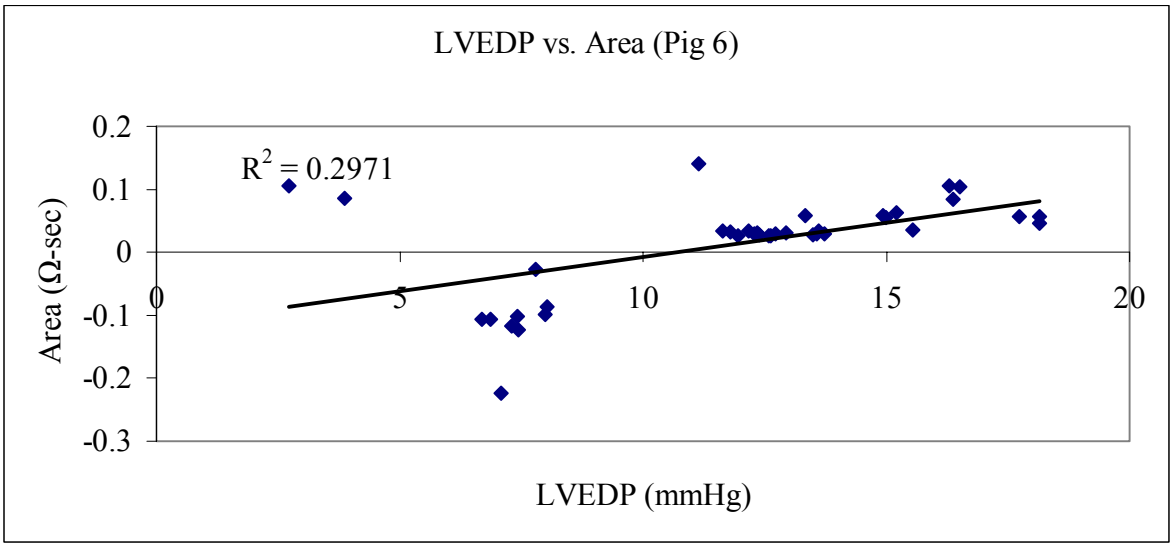

Figure 40

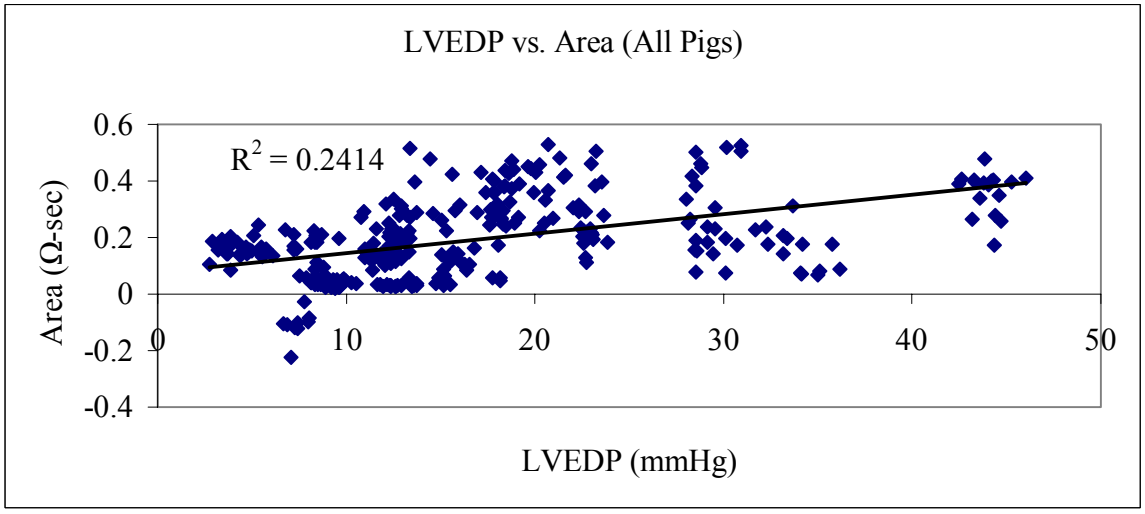

Figure 41

Figures 40 and 41: Showing the relationship between left ventricular end diastolic pressure (LVEDP) and the area under the intra-cardiac Z curve (depicted as Area in graph). Figure 40 shows results from a selected pig and 41 of all pigs.

4.6.9. Relationship Between Intra-cardiac Bioimpedance (Area Under Curve) and Stroke Volume

The stroke volume was calculated as the quotient of the measured cardiac output and heart rate and then plotted against the area under the curve of the intra-cardiac Z. There was a very poor correlation between the two in our measurements (R^2=0.0545).

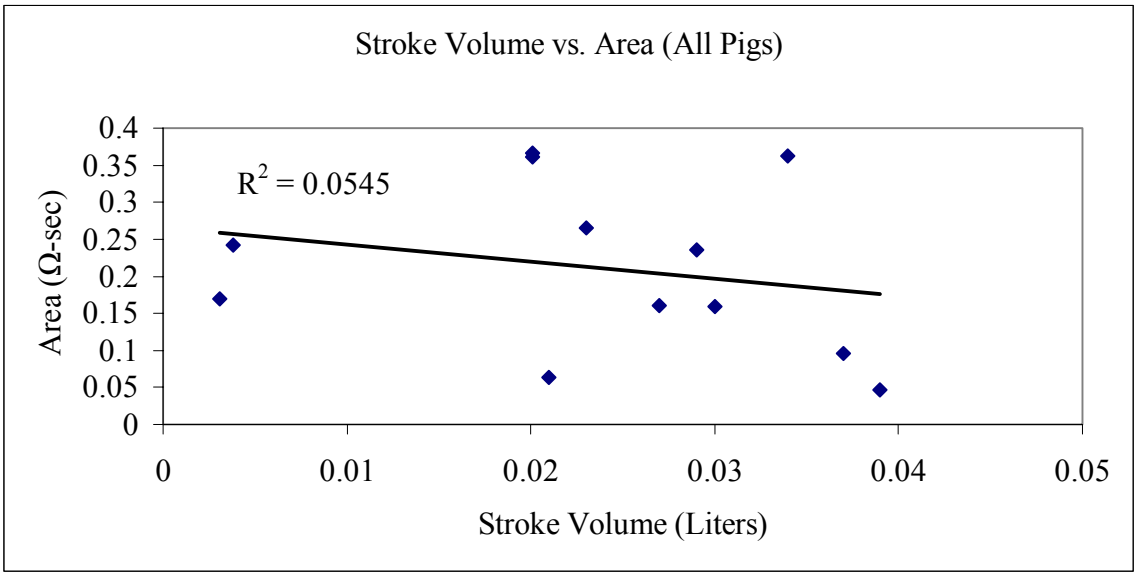

Figure 42: Shows no correlation between stroke volume and area under the intra-cardiac Z curve.

5. Discussion

Fluid overload was used as an indication of heart failure in these experiments. It was determined by changes in hemodynamic parameters as follows: Reduction of cardiac output and aortic pressure, an increase in pulmonary artery pressure (PAP), pulmonary capillary wedge pressure (PCWP) and central venous pressure (CVP) against bioimpedance measurements. Verapamil acts by blocking voltage-gated calcium channels in the heart and thus inhibiting calcium influx thereby reducing contractility and impairing AV conduction by elongating the atrioventricular (AV) time. Metoprolol is a selective ß 1 inhibitor which causes a decrease in cardiac output, heart rate, central sympathetic activity and impairs AV conduction. The negative inotropic effect of Verapamil and Metoprolol led to a decrease in both cardiac output and blood pressure (see figure 10). Cardiac output reduction together with fluid overload led to a congestion in venous and pulmonary systems leading to a rise in PCWP, mean PAP and CVP. Critical hemodynamic instability led to application of calcium, atropine and catecholamines for stabilization where necessary.

Effect of Electrode Position

The placement of electrodes in impedance measurement determines the type of resulting signal (see results figures 16 - 19). In the subcutaneous placement, a good respiration signal is recordable with the cardiac impedance signal visible on filtering. With the placement of electrodes both intra-cardiac and subcutaneous, a low frequency respiration signal is recordable and composed of higher frequency cardiac components. A pure intra-cardiac signal results when all electrodes are placed in the heart. The respiratory component is visible by low-pass filtering. The reason for these different signal entities probably lies in the favorable paths of the electric current relative to the electrodes. In the heart, the pulsatile cardiac action supersedes the respiratory chest movements locally and thus leads to the intra-cardiac signal being more dominant compared to the respiratory impedance signal. The reverse is true for the subcutaneous measurement where respiratory movements dominate. Placement of electrodes both intra-cardiac and subcutaneous generates a combined signal. The changes in intra-cardiac Z most probably result from changes directly related to blood flow and flow of electric current in relation to the Z electrodes. The intra-cardiac electrodes in these experiments were placed in the right atrium (RA), right ventricle (RV) and coronary sinus (CS). Differences should therefore be evident on the intra-cardiac Z signal whenever there are

physiological changes in the heart which would interfere with the direct flow of current between these electrodes along the shortest most conductive path (blood flow in this case). The recorded Z by use of intra-cardiac electrodes alone had two peaks (see results figure 29); the first corresponding with the P wave and the second to the QRS complex. The first peak probably resulted from the interruption of the flow of blood between the RA and the CS due to pressure increase in the RA. This increase in pressure presses the mouthing of the CS against the RA wall and so closing it during RA filling. The tricuspid valve then opens and causes a direct flow between RA and RV, thus decreasing Z. During ventricular ejection, the tricuspid valve closes. This interference of direct blood flow between the electrodes causes another peak of Z. The Z signal then falls, reaching an all time minimum almost coinciding with the T-wave during ventricular repolarization. The conductivity of blood is increased from ventricular end-diastole to end-systole due to massive blood flow and hence a decrease in Z. The inverted relationship of the intra-cardiac Z and LV pressure maxima and minima (figure 29) is reminiscent of the relationship between left ventricular volume maxima and minima and LV pressures. This suggests that the intra-cardiac impedance could be a reflection of volumetric changes in the ventricle. This is further strengthened by the fact that more pronounced cardiac features are recordable by placement of two electrodes in the RV and two subcutaneously compared to placement of an electrode each in RV and CS, and two subcutaneously. The respiratory signal is also sometimes detectable in the intra-cardiac impedance signal. This could be the result of intra-thoracic pressure changes which change the size of the mediastinum and the flow of blood within and around it.

Factors Affecting Bioimpedance

The exact origin of measured thoracic bioimpedance is still unclear (35). Soft tissues, hydration state, surface fat, lung fluid, lung air and major vessels all play a role. There is no published data showing the exact contribution of different thoracic tissues in live animals or humans, but apparently different body tissues contribute differently (27). Mean pulmonary impedance was consistently increasingly lower with an increase in fluid overload, with maximal mean impedance being at the baseline and minimum at the second fluid load (fl2) in our studies. Increase in pulmonary fluid content is associated with an increase in conduction (29, 36 - 44). Fluid congestion leads to an increase in pulmonary artery pressure (PAP) which is the hydrostatic driving pressure for pulmonary edema. On the other hand, a reduced function of the left heart causes an increase in

mean left atrial pressure and consequently pulmonary capillary wedge pressure (PCWP) also resulting in an increase of plasma and fluid in the lungs. The increase in fluid results in a decrease in Z, hence the applicability of this method in measuring pulmonary congestion and heart failure. The validity and reliability of data generated is subject to further investigation.

The rate of the respiratory Z signal has a one to one relationship with the respiratory rate (see results figure 23). Changes in pulmonary Z correlate with tidal volume (29, figures 26, 27 and 28). In this study, high tidal volume (TV) was associated with a maximum delta Z and low a minimum. The strong correlation between magnitude of Z signals and TV suggest delta Z as a result of changes in TV. This could be the result of decreased conductivity due to increased air content of the lungs or due to displacement of intra-thoracic vessel fluid and / or compression of vessels by the increase of intra-thoracic pressure resulting from inspiration. Davidson et al. (45) used weight-rated impedance results to predict tidal volumes in rats with significant results ($R^2 \geq 98\%$). The correlation of Z with CO (figure 14, $R^2=0.83$) in our study suggests that congestion leads to change in the average Z (46). If tidal volume is unchanged, then the change in average Z is the result of congestion. The non-linear relationship between CO and Z could probably be explained by other factors affecting the Z signal, e.g. respiration.

The lung´s resistivity is about seven times that of blood (27). In that case;

$$\frac{RB \times RL}{RB + RL} = \sim RB$$

Formula depicting the relationship of resistivities of blood and lung.

RB = Resistivity of blood

RL = Resistivity of lung.

This makes blood the preferred route of conduction. The waves of most of the other measured thoracic parameters move in phase with Z when put on a low pass filter. Impedance, ventilation, AO and LV pressures were in phase with each other suggesting the modulation of these parameters by intra-thoracic changes during ventilation. This is due to the non-compliance of the aorta and the LV. The ECG on the other hand has a vertically inverted image. This could be because the ECG is a recording of spreading electrical currents originating from the heart and, unlike Z, is therefore a factor of conductivity. On the other hand, the high lung resistivity (poorer lung conductivity) would

also be reversed by pulmonary congestion leading to a decrease in bioimpedance. The degree to which thoracic air influx and fluid displacement each affect the value of bioimpedance warrants further investigation.

Whereas the right heart and the central venous system are highly compliant, the left heart and aorta are rigid. This means relatively small pressure changes in the right heart and central veins are associated with large volumetric changes, unlike in the left heart and aorta where changes are minimal. Therefore volume related Z changes reflect changes in the right heart. This could be related to pressure changes in a normal heart where the Frank-Sterling mechanism still applies. In the case of our experimental pigs, this mechanism can no longer be assumed to be fully applicable after Verapamil and Metoprolol application due to the contractility effects of these drugs. That is probably why the Z here was not correlating with ventricular pressures and stroke volume as would otherwise be expected. Though the measurement of intra-cardiac Z was not the primary objective of this study, the correlation of intra cardiac Z and heart rate suggests beat related changes of Z (see results section figures 29 and 30). The heart pumps blood which can be electrically viewed as a mass of conducting ions. This leads to a fall in Z.

Metry et al (23) evaluated the effects of age and sex in transthoracic bioimpedance in 111 healthy subjects. This group consisted of 55 males and 56 females aged between 20 and 69 years. They found out that female impedance was higher than that of males but this difference became insignificant in the 6^{th} decade of life.

The change in total thoracic impedance over time can be given by the equation (14)

$$\Delta Z = \frac{(Z0 - Zi)}{Z0}$$

Formula depicting the change in total thoracic impedance over time.

Z0 = baseline thoracic impedance (ohm)

Zi = thoracic impedance at time interval i

ΔZ = relative change in thoracic impedance

The effect of sex in impedance could be explained by the fact that females generally have a smaller cross-sectional chest area (impedance is inversely proportional to cross-sectional area), smaller blood volumes and a higher fat/muscle ratio (the resistivity of fat is higher than that of muscle (27

and table 3)). These factors affect Z0 and therefore the relative change in thoracic impedance as demonstrated by the above equation. Paradoxically, males generally have larger lung volumes than females which should be associable with higher thoracic impedances.

Studies Involving the Use of Bioimpedance in Measuring Lung Fluid

Several studies have confirmed the viability of using pulmonary bioimpedance to measure changes in lung fluid (15, 14, 29, 36 - 44, 46 - 51). Nierman et al. (29) compared lung fluid changes measured by bioimpedance to postmortem gravimetric measurements after acute lung injury in a porcine endotoxin model. In this study, a good correlation was observed (R^2=0.81). Wang et al. (52) used a canine model of pacing induced heart failure by applying rapid pulses of 240 pulses per minute. This showed a reduction in the mean impedance of 10.6±8.3% and was reversible on termination of pacing showing the viability for chronic use.

Some investigators have suggested the use if bioimpedance in estimating extra-vascular lung water (14, 51). Spinale et al. (51) compared thoracic impedance with double dilution and thermal dilution to estimate extra-vascular lung water in nine anesthetized dogs after induction of pulmonary injury with oleic acid. They found a strong correlation between double dilution and impedance ($r = 0.7$, $p<0.05$). They concluded that bioimpedance could be used for non-invasive measurement of extra-vascular lung water. An increase in thoracic fluid conductivity was found in peripartum women with both preeclampsia and pulmonary edema as compared with those without by Newman et al. (53). These investigators could establish a significant difference in conductivity between those with mild and those with severe preeclampsia (mean 53.3 kohm-1 against 62.8 kohm-1). When thoracentesis was performed on patients with pleura effusions, Zehrahn et al. found a change of trans-thoracic impedance of 2.3 ohm/l aspirated fluid from the baseline (54). These changes were found to be variable depending on underlying disease. Zellner et al. induced an acute lung sepsis in seven pigs by infusion of Pseudomonas aeruginosa and concluded that impedance can provide a relatively simple and reliable method of continuously monitoring changes in extra-vascular lung water in the ICU (14). They observed that bioimpedance may fail to accurately detect small changes in extra-vascular lung water. On the other hand, Raaijmakers et al. described different results from cardiogenic and non-cardiogenic edema in humans (55). Whereas cardiogenic edema caused an increase in pulmonary impedance, non-cardiogenic caused a decrease. These investigators

explained the differences as being due to the increase of protein / albumin in non-cardiogenic edema.

Viability of Bioimpedance to Monitor Heart Failure in Humans Compared to Routine Methods

Trans-thoracic Z has been used in different studies to monitor heart failure in humans (48, 49 and 56). Zlochiver et al. (48) established a significant difference in lung resistivities of congestive heart failure patients compared to healthy volunteers. These results suggested the viability of bioimpedance to monitor medication dosage on a frequent basis in congestive heart failure. Bioimpedance also increases in CHF patients during diuresis (49). Current methods of establishing the adequacy of diuresis include chest radiographs, improvement of clinical symptoms and weight control. X-ray has proved insensitive in differentiating cardiomegaly from abnormal pulmonary fluid as compared to bioimpedance (46) and cannot effectively differentiate between pulmonary edema and atelectasis (51). Shochat et al. established that X-ray can detect interstitial edema before it develops into the clinically relevant alveolar edema (15). Measurements of body weight changes can be inaccurate because these do not necessarily result from changes in lung water. Improvements in cardiac function can result in decrease in lung water which is not necessarily accompanied by decrease in total body fluid (49). Nescolarde et al. more recently performed segmental thoracic impedance in 25 patients undergoing ambulatory peritoneal dialysis (35). They established that the current measurement methods of establishing tissue water content and distribution were expensive, invasive and had limited accessibility. Bioimpedance on the other hand was a cheaper and simpler alternative for clinical assessment of ambulatory peritoneal dialysis patients. Other measurement methods include radioactive isotope imaging, computed axial tomography, hydrodensitometry, dual energy x-ray absorbimetry (DEXA), magnetic resonance imaging (MRI) and neutron activation analysis.

Packer et al. (56) used impedance to predict clinical worsening in ambulatory heart failure patients by evaluating 212 patients who had recently had a clinical decompensation. These patients underwent serial clinical evaluation and blinded impedance cardiographic testing every 2 weeks for 26 weeks. Follow-up was conducted after death or mandatory re-hospitalization. They concluded that when performed regularly in recently decompensated heart failure patients, impedance cardiography can identify patients with an increased risk of re-decompensating. In clinical practice,

heart failure is recognized from congestion signs although it is now evident that these do not demonstrate severity of heart failure and their absence does not mean normal ventricular filling pressure (16). Some patients with heart failure do not show clinical features and are therefore at risk of inadequate diagnosis and therapy. Stevenson and Perloff (57) found out that rales, edema and elevated jugular venous pressure were absent in 42% of their 50 patients and physical evidence for congestion absent in 44% of patients with a PCWP of 35 and above. In a study of 52 pre-transplantational patients, Chakko et al. found out that physical and radiological signs were present in patients with a high PCWP but not in those with a relatively lower one (16). They found out that interstitial and pulmonary edema had poor predictive value for patients with a PCWP greater or equal to 30 mmHg and that radiological pulmonary congestion was absent in 35% of patients. However, there was a good correlation between right atrial pressure and PCWP. Shochat et al. monitored 403 patients hospitalized for acute coronary syndrome with thoracic bioimpedance (15). They could establish that in 70% of patients who subsequently developed heart failure, internal thoracic bioimpedance decreased by 16.4% compared to 4.5% in those who did not. The values of these patients normalized after resolution of pulmonary edema. These investigators concluded that continuous monitoring of bioimpedance can detect heart failure in the preclinical stage and that a decline of more than 12% in monitored patients was associated with development of acute heart failure in 97.5% of cases. Direct measurement of hemodynamics may be helpful in patients whose physical examination is not possible or not concordant with symptoms. Current methods of hemodynamic monitoring of heart failure patients include pulmonary artery catheter (PAC), B-type natriuretic peptide (BNP) and echocardiography. PAC is not routinely used in management of HF patients but is useful in recurrent or medically refractory heart failure. BNP is important in determining the etiology of dyspnea in emergency patients who have no previous diagnosis of heart failure. It is also good for prognosis but its use is not yet routine. Echocardiography is good for determining ventricular function and size and monitoring hemodynamic parameters.

Bioimpedance (Z) as a hemodynamic monitoring tool has several advantages: It is cheaper, less risky, easy to use in the ambulatory situation, non-invasive, usable continuously, operator independent, simple to operate and widely applicable in different clinical settings (58). This system of monitoring does not necessarily need a clinician, is associated with reduced mortality and morbidity (49), does not use harmful ionizing radiation and little time is needed for set up and use. There are reports of times between 3.2 – 4.6 minutes needed for set up and 8.4 patients (compared

to 12.9 patients needed by supra-sternal doppler ultra sound) to get enough experience required for satisfactory results (59). The disadvantages of pulmonary artery catheter (PAC) in hemodynamic monitoring include invasiveness, difficulty in insertion, high cost and the fact that data are not always understood or well responded to (59). The ESCAPE study investigators (60) established that therapy to reduce volume overload during hospitalization for heart failure led to improvement of signs and symptoms of elevated filling pressures both with and without PAC and concluded that PAC was associated with anticipated adverse effects. They suggested research on non-invasive assessment possibilities which could be used to better tailor therapy. Methods other than bioimpedance for estimating cardiac output (CO) include echocardiography, pulse contour analysis, ventriculography, thermodilution, and the direct and indirect Fick methods (61). The indirect Fick method utilizes carbon dioxide (CO2) production after re-breathing to estimate CO. This is only applicable in ventilated patients. Thermodilution in PAC using single measurements is quite inaccurate (22% error) which can be reduced to 13% by averaging triple measurements. Although thermodilution has established itself well in the measurement of CO, it still largely relies on the user technique (injecting technique, timing of injection in dependence to respiratory circle, number of CO values taken and injectate temperature). Pulse contour analysis is becoming increasingly popular in the ICU but it requires femoral artery access and can therefore not be readily used. Esophageal Doppler is invasive and requires sedation of the patient whereas echocardiography is operator dependent and usable only intermittently. Intense monitoring is of benefit to sick patients in early stages of illness. A less user dependent and less invasive measurement technique is therefore necessary.

Use of Bioimpedance in Measuring Cardiac Output

Cardiac output monitoring with Z is becoming increasingly popular. It is comparable to invasive methods e.g. direct and indirect Fick methods and thermodilution as shown by numerous publications (62 - 64). Belardinelli et al. compared bioimpedance with Fick and thermodilution methods in measuring cardiac output. In 25 patients who had CAD and had had MI, they found a high correlation between both methods (62). Shoemaker et al. did a multi-center trial on 68 critically ill patients comparing impedance cardiac output with thermodilution with good correlation of both methods (63). After a study on 191 patients who had had a right heart catheter, the COST study arrived at similar results in an abstract confirming its reliability in measuring CO (64). On the

other hand, some investigators have questioned the accuracy of bioimpedance in measurement of cardiac output. Wang et al. claimed that there is a poor correlation between current generation impedance cardiography (ICG) devices and invasive measurements of cardiac output (65). These researchers suggested that ICG should be limited to the research setting. Its accuracy in patients with pulmonary edema (66) and post thorax operations (67, 68) have been found dissatisfactory. In a study of 50 patients after coronary bypass surgery, Sageman et al. found a poor correlation due to distortion of their anatomy and the presence of tubes in their thoraces (67). Doering et al. also found a poor correlation in cardiac surgery patients (68). Diminished accuracies have been reported in patients with low baseline Z (59) and those with excessive conductive material, e.g. water, intercostal catheters, pleural effusions, severe CHF, hemothorax and severe pneumonia. In patients with excessive conductive material, better conductive routes than the aorta are associated with the miscorrelation. Electric current travels preferably through these alternative routes than the normal path of aorta. Each contraction of the left ventricle (LV) causes the aorta to expand, causing a decrease in Z due to an increase in volume in a manner proportional to stroke volume. These pulsatile changes in Z are used to derive CO. Bioimpedance therefore has a good potential for being a monitoring tool even over longer periods of time.

Future Work

Bioimpedance measurements could therefore serve as a basis for a heart failure monitoring system in future. Such a system could possibly consist of a pacemaker sized device that is implantable on heart failure patients´ chests under local anesthesia and minimally invasive conditions. Such a device could use bioimpedance by measuring the thoracic electrical resistance and detecting its change due to conditions leading to reduction in electrical resistance, e.g. pulmonary edema, by congestive heart failure. In the case of worsening congestion by heart failure, the system alerts both the patient and the responsible medical practitioner. Data is transmitted by telemetry to the practitioner who, judging from the values, readjusts medication of the patient accordingly and so intervenes before debilitating deterioration leads to mandatory hospitalization for adequate therapy. Since hospitalization from congestive heart failure is in many cases mandatory and hospitalization generally is the most costly item of healthcare systems of most western countries, this money could be diverted to research and provision of better healthcare. Such a system would also address the shortage of doctors in many countries, since more patients per doctor can be catered for. At the

same time, the quality of life of the patient is improved, i.e. less hospitalization, less visits to health care centers and a generally better sense of well-being. Telemetry could make use of common communication tools used in telemonitoring, e.g. via telephone or internet.

Future work should determine long term stability and functionality, patient tolerance, reliability and biocompatibility. Improvement of telecare and home monitoring with special training of healthcare personnel and development of telecare centers or integration of telecare to family/general practitioner clinics would enable an effective functioning of the home monitoring system.

The establishment of norm values according to age, sex, body size, weight and underlying pathology is necessary since these factors greatly influence the magnitude of the measured impedance signal. It would also be important to establish the individual importance of the amplitude or the area under the impedance curve as well as a suitable time interval and duration of measurement recording. Applications in other medical fields such as monitoring of dialysis patients, intensive care monitoring etc. should also be investigated.

The combination of hemodynamic monitoring and telecare would benefit patients suffering from heart failure that are at home or in remote areas. Its integration into the routine health care management system may require time as initial financing and skepticism from healthcare professionals is to be expected. The current developments in telecommunication and internet technologies would ensure the functionality of such a system. The establishment of a threshold impedance value which can be considered pathological and its rating according to desired patient categories e.g. by age, sex, body size, weight etc, will be necessary.

The possible future applications of intra-cardiac Z could be the use of the time derived from atrial and ventricular contractions to determine the ‘optimal’ time for dual chamber pacemakers. The best atrioventricular (AV) delay to optimize cardiac hemodynamics is still yet to be derived despite current advanced state of dual-chamber pacemaking. Intracardiac impedance could be used to optimize energy consumption by optimally setting the pulse width and amplitude in pacemakers (69). Ventilation controlled pacemakers could be developed by utilizing intra-cardiac impedance signals after low pass filtering. Several studies have shown the improvement of exercise capability in patients with pacemakers by adjusting the rate; and for this trans-thoracic impedance measurements can be used as suggested by Alt et al. (70). These investigators also suggested that respiratory minute volume is more precise for rate controlled pacemakers than tidal volume or respiration rate alone and that trans-thoracic impedance is appropriate to measure respiratory minute

volume. Valvular, mural and other blood flow defects in the heart and circulatory system could also be detectable using Z.

Conclusion

The results of this research work show that local subcutaneous bioelectrical impedance (Z) correlates with respiration parameters (tidal volumes and respiration rates), fluid overload (fl) and cardiac output (CO) and could therefore serve as an indicator for changes in hemodynamic status. A good application could be in heart failure where lung congestion occurs. Although the results of this particular porcine study may be limitedly applicable to humans, there are currently numerous studies proving its applicability to humans. If applied, this method of hemodynamic monitoring could lead to an improvement of quality of life, less mortality and less hospitalization and associated costs. Fluid management associated with minimizing extravascular lung water has been associated with fewer ICU days and less use of mechanical ventilation. Recent publications have shown that bioimpedance could be used to predict congestion in congestive heart failure patients prior to hospitalization and suggest its application to modify medical titration during worsening congestion (50). Monitoring of advanced pulmonary disease could also be a possible application. Non-invasive monitoring could be used in the ICU, emergency room, the general ward, the out-patient clinic and in the home care unit.

Hemodynamic monitoring provides reassurance that right diagnosis and therapy has been established. Bioimpedance is cheaper than PAC in terms of equipment and also because it can be used in the home setting to prevent hospitalization. It is also easy to use, but instances of false alarms in intensive care typical of continuous monitoring are set to increase and so are the associated caregiver burn-out syndromes.

Telemonitoring allows monitoring of physiological variables measured in patients at home by physicians and caregivers by making use of standard telecommunication technology e.g. telephone, cable etc. There is good evidence that home-based telemedical care can reduce readmission rates and hospitalization length in heart failure cases (30, 32, 61). It has the capacity to optimize therapy, promote appropriate use of financial resources, enhance quality of care of the patient and avoid risks associated with hospitalization.

6. Summary

Congestive heart failure (CHF) is associated with an enormous human and economic burden. This is due to resulting high mortality, progressive and prolonged morbidity and recurrent hospitalization.

A large portion of the costs arises from mandatory hospitalization and re-hospitalization for decongestion. Adjusting medication in early stages of deterioration could improve long term outcome, reduce re-hospitalization rates and costs. The current diagnostic and monitoring procedures for heart failure patients have two major setbacks: First, they are incapable of predicting preclinical decompensation. This leads to the disease being diagnosed so late that hospitalization becomes mandatory. Secondly, they are not routinely usable in the home setting by heart failure patients. A system which is free of these setbacks is currently not readily available. Bioimpedance in conjunction with telemedicine offers a possible solution.

Bioimpedance (Z) is the resistance of biological tissue to electric current. The lung has unique electrical properties: The air inside acts as an insulator, the alveoli as capacitors and blood as a good conductor. The circulatory close proximity of the lung and the heart makes the lung sensitive to fluid overload. These unique properties make bioimpedance monitoring of the lung viable. Accumulation of fluid during pulmonary edema results in a measurable reduction of the Z. This was used as the basis of this study.

Telemonitoring allows monitoring of physiological variables measured in patients at home by physicians and caretakers by making use of standard telecommunication technology e.g. telephone, cable etc. This would allow the close monitoring of heart failure patients and facilitate early intervention in case of worsening and so prevent hospitalization. Consequently, rates of admission to hospital would be reduced and discharge accelerated. The epidemiological and financial significance of heart failure predicts home care as a cost-effective solution with a good potential. The viability of both telemedicine in monitoring patients at home and bioimpedance in monitoring heart failure has been examined separately in numerous publications.

Aim of this study was to determine if local thoracic bioelectrical impedance (Z) correlates with respiration parameters (tidal volumes and respiration rates), fluid overload (fl) and cardiac output (CO) and could therefore serve as a basis for a heart failure monitoring system.

In seven juvenile farm pigs (average weight 32.5±5 kg), a subcutaneous passive can with four electrodes was implanted on the left side of the chest. After obtaining baseline values, acute heart

failure and fluid overload were induced in two steps (reduction of CO to 70-80% and then to 50-60% of baseline value) by gradual injection of 4.3±2.0 mg Metoprolol and Verapamil for each step together with fluid administration (259±72ml 0.9% saline and 6% hydroxyethyl starch each for each step).

Stepwise injection of Metoprolol, Verapamil and fluid resulted in a reduction of cardiac output, LVEF and MAP and an increase in MPAP, PCWP and CVP.

The percentage change in Z decreased from baseline to the first and second step of fluid load. A linear trend was found for this decrease (R^2=0.83)

Several studies have confirmed the viability of using pulmonary electrical impedance to measure changes in lung fluid both in humans and animals with results in conformation with those of this study. The results of this research work show a possibility of measuring lung fluid content by thoracic bioelectrical impedance as a possible parameter of non-physiological changes in lung fluid. A good application could be in heart failure where lung congestion occurs. Although the results of this particular porcine study may be applicable to humans to a limited extend, there are currently studies confirming its applicability to humans. If applied, this method of hemodynamic monitoring could lead to an improvement of quality of life, less mortality and less hospitalization and associated costs.

7. Zusammenfassung

Herzinsuffizienz ist eine der führenden Ursachen von Mortalität und Morbidität in Industrieländern und gehört zudem zu den kostenintensivsten Krankheitsbildern. Der größte Teil dieser Kosten entsteht als Folge von Krankenhausaufenthalten und Wiedereinweisungen zur kardialen Rekompensation. Eine Anpassung der medikamentösen Therapie im Anfangsstadium der Dekompensation könnte ggf. das Fortschreiten der Dekompensation verhindern. Dies würde wiederum die Anzahl der Krankenhauseinweisungen als auch die Kosten reduzieren. Die bisher verfügbaren ambulanten Überwachungsmaßnahmen haben verschiedene Nachteile: die Erkennung der Dekompensation erfolgt oft erst relativ spät bzw. die „Vohersagen" der Dekompensation erfolgt nicht sicher. Die bisherigen technischen Geräte sind oft für die ambulanten routinemäßige Anwendung für Patienten zu komplex und für die Anwendung/Auswertung wird speziell geschultes Personal benötigt.

Bioimpedanz („Z") ist der Widerstand biologischer Gewebe zu Wechselstrom. Durch die kardiale Dekompensation kommt es zu einer Veränderung des Flüssigkeitsgehaltes des Gewebes und damit zu einer Änderung der Bioimpedanz. Die Flüssigkeitsstauung beim Lungenödem verursacht eine Abnahme der messbaren Bioimpedanz. Dieser Effekt wurde als Basis für diese Studie verwendet.

Ziel dieser Arbeit war zu untersuchen, ob eine subkutane erfasste bioelektrische Impedanz (Z) mit Beatmungsparameter (Atemminutenvolumen und Atemfrequenz), Flüssigkeitsbelastung (fl) und Herzminutenvolumen (CO) korreliert und so als Basis für ein implantierbares Herzinsuffizienzüberwachungssystem dienen kann.

Ein subkutanes Elektrodenelement mit Messelektroden wurde in die linken Thoraxhälften von sieben Schweine (Gewicht 32.5±5 Kg) implantiert. Nach der Aufzeichnung von Basiswerten, wurde eine Flüssigkeitbelastung (als Simulation einer kardialen Stauung/Dekompensation) in zwei Schritten (Reduktion des Herzzeit Volumens auf 70-80%, und dann auf 50-60% der Basiswerte) induziert. Diese erfolgte durch eine langsame Injektion von Metoprolol, Verapamil (jeweils 4.3±2.0mg für die erste und zweite Flüssigkeitsbelastungsstufe), physiologischer Kochsalzlösung und sechsprozentiger Hydroxyethylstärke (259±72ml für die erste und zweite Flüssigkeitsbelastungsstufe).

Schrittweise Injektion von Metoprolol, Verapamil und Flüssigkeit führte zu einer Abnahme des Herzminutenvolumens (CO) und des mittleren arteriellen Drucks (MAP); und zu einer Zunahme

des mittleren pulmonaren arteriellen Drucks (MPAP), des pulmonären Kapillardrucks (PCWP) und des zentralen venösen Drucks (CVP). Die prozentuale Abnahme von Z von Baseline, erste und zweite Flüssigkeitsbelastungsstufe folgte einem linearen Trend (R2 = 0.83).

Diese Ergebnisse zeigen die Möglichkeit, Veränderung in Lungenflüssigkeitsmengen mittels subkutan erfasster Bioimpedanz zu messen. Ein mögliches Anwendungsgebiet wäre die Detektion von Veränderungen im Lungenflüssigkeitsvolumen als Indikator einer beginnenden kardialen Dekompensation.

8. References

1. Hunt et al. ACC/AHA Guidelines for the Evaluation and Management of Chronic Heart Failure in the Adult: Executive Summary A Report of the American College of Cardiology/American Heart Association Task Force on Practice Guidelines (Committee to Revise the 1995 Guidelines for the Evaluation and Management of Heart Failure). Circulation. 2001; 104:2996-3007.
2. M. Malek. Health Economics of Heart Failure. Heart. 1999; 82: 11iv-13.
3. Barry Massie, Nihir Shah. Evolving Trends in the Epidemiologic Factors of Heart Failure: Rationale for Preventive Strategies and Comprehensive Disease Management. Am Heart J. 1997; 133: 703-12.
4. JJ. McMurray, S. Stewart. Epidemiology, Etiology and Prognosis of Heart Failure. Heart. 2000; 83:596–602
5. Martin R. Cowie. Annoted References in Epidemiology. European Journal of Heart Failure. 1999; 101-107.
6. Christian Mewis, Reimer Riessen, Ioakim Spyridopoulos. Kardiologie Compact. Thieme Verlag. 2004; 230-280.
7. T. Rydén-Bergsten, F. Andersson. The Health care Costs of Heart Failure in Sweden. J Intern Med. 1999; 246 (3): 275–284.
8. Neumann et al. Heart Failure: the Commonest Reason for Hospitalization in Germany—Medical and Economic Perspectives. Dtsch Arztebl Int. 2009; 106(16): 269-75.
9. Vinson et al. Early Readmission of Elderly Patients with Congestive Heart Failure. J Am Geriatr Soc. 1990; 38:1290-5
10. Nadas et al. Pedriatic Aspects of Congestive Heart Failure. Circulation. 1960; 21:95-111.
11. Ursula Maria Schmidt-Ott, Deborah Davis Ascheim. Thyroid Hormone and Heart Failure. Current Heart Failure Reports. 2006; 3:114-119.
12. Vasan et al. Plasma Homocysteine and Risk for Congestive Heart Failure in Adults Without Prior Myocardial Infarction. JAMA. 2003; 289:1251-1257.
13. Wong et al. Retinopathy and Risk of Congestive Heart Failure. JAMA. 2005; 293: 63-69.
14. Zellner et al. Bioimpedance: A Novel Method for the Determination of Extravascular Lung Water. J Surg Res. 1990; 48: 454-459.

15. Shochat et al. Internal Thoracic Impedance Monitoring: A Novel Method for the Preclinical Detection of Acute Heart Failure. Cardiovascular Revascularization Medicine 2006; 7: 41-45.
16. Chakko et al. Clinical, Radiographic and Hemodynamic Correlations in Chronic Congestive Heart Failure: Conflicting Results may Lead to Inappropriate Care. Am J Med. 1991; 90: 353–359.
17. SHEP Cooperative Research Group. Prevention of Stroke by Antihypertensive drug Treatment in Older Persons with Isolated Systolic Hypertension. Final Results of the Systolic Hypertension in the Elderly Program (SHEP). JAMA. 1991; 265(24):3255-64.
18. Dahlof et al. Morbidity and Mortality in the Swedish Trial in Old Patients with Hypertension (STOP-Hypertension). Lancet. 1991; 338(8778):1281-5.
19. SOLVD Investigators. Effect of Enalapril on Mortality and the Development of Heart Failure in Asymptomatic Patients with Reduced left Ventricular Ejection Fractions. N Engl J Med. 1992; 327:685-691.
20. Pfeffer et al. Effect of Captopril on Mortality and Morbidity in Patients with left Ventricular Dysfunction After MI. Results of the Survival and Ventricular Enlargement Trial. N Engl J Med. 1992; 327:669-77.
21. AIREX Study Investigators. The Follow up Study of Patients Randomly Allocated Ramipril or Placebo for Heart Failure After Acute Myocardial Infarction: AIRE Extension Study. Lancet. 1997; 349: 1493-97.
22. Gregory D. Lewis, Marc J. Semigran. The Emerging Role for Type 5Phosphodiesterase Inhibitionin Heart Failure. Current Heart Failure Reports. 2006; 3:123-128.
23. Metry et al. Gender and age Differences in Transthoracic Bioimpedance. Acta Physiol Scand. 1997; 161:171-175.
24. Kuusik et al. New Synchronous Measurement Technique for Intracardiac Impedance Analysis. International Journal of Bioelectromagnetism. 2003; 5: 23-24
25. Gabriel et al. The Dielectric properties of Biological Tissues: III. Parametric Models for the Dielectric Spectrum of Tissues. Phys Med Biol. 1996; 41: 2271 – 2293.
26. Christopher W. Gregory. Use of Charge-Charge Correlation in Impedance Measurements: Test of the EPET Method. Dissertation 2005. Morgan Town, West Virginia. Pages 1-19

27. Jaakko Malmivuo, Robert Plonsey. Bioelectromagnetism - Principles and Applications of Bioelectric and Biomagnetic Fields, Oxford University Press, New York, 1995. Chapter 7. Internet-version. http://butler.cc.tut.fi/~malmivuo/bem/bembook/07/07.htm
28. Gabriel et al. The Dielectric Properties of Biological Tissues. Phys Med Biol. 1996; 41(11): 2231-49
29. Nierman et al. Transthoracic Bioimpedance Can Measure Extravascular Lung Water in Acute Lung Injury. J Surg Res. 1996; 65(2): 101-8.
30. Louis et al. A Systematic Review of Telemonitoring for the Management of Heart Failure. The European Journal of Heart Failure. 2005; 5: 583-590
31. Scherr et al. Mobile Phone-based Surveillance of Cardiac Patients at Home. Journal of Telemedicine and Telecare. 2006; 12 (5): 255-261(7).
32. Martinez et al. A Systemic Review of the Literature on Home Monitoring for Patients With Heart Failure. Journal of Telemedicine and Telecare. 2006; 12 (5): 234-241.
33. Ohlsson et al. Continuous Ambulatory Hemodynamic Monitoring With an Implantable System. European Heart Journal. 1998; 19: 174-184.
34. T. D. V. Swinscow, M. J. Campbell. Statistics at Square One, 10th Edition (2002). 111 – 125.
35. Nescolarde et al. Thoracic Versus Whole Body Bioimpedance Measurements: The Relation to Hydration Status and Hypertension in Peritoneal Dialysis Patients. Physiol. Meas. 2006; 27: 961-971.
36. Pomerantz et al. Transthoracic Electrical Impedance for the Early Detection of Pulmonary Edema. Surgery. 1969; 66 (1): 260-268.
37. Pomerantz et al. Clinical Evaluation of Transthoracic Electrical Impedance as a Guide to Intrathoracic Fluid Volumes. Ann. Surg. 1970; 171 (5): 686-694.
38. Van De Water et al. Pulmonary Extravascular Water Volume: Measurement and Significance in Critically ill Patients. J. Trauma. 1970; 10 (6): 440-449.
39. Van de Water et al. Impedance Plethysmography. A Noninvasive Means of Monitoring the Thoracic Surgery Patient. J. Thoracic Cardiovasc. Surg. 1970; 60 (5): 641-647.
40. Berman et al. Transthoracic Electrical Impedance as a Guide to Intravascular Overload. Arch. Surg. 1971; 102 (1): 61-64.
41. Luepker et al. Transthoracic electrical Impedance: Quantitative Evaluation of a Noninvasive Measure of Thoracic Fluid Volume. Am. Heart J. 1973; 85 (1): 83-93.

42. Ramos et al. Transthoracic Electric Impedance. Minnesota Med. 1975; 58: 671.
43. Haffty et al. A Clinical Evaluation of Thoracic Electrical Impedance. J. Clin. Eng. 1977; 2: 107-116.
44. Fein et al. Evaluation of Transthoracic Electrical Impedance in the Diagnosis of Pulmonary Edema. Circulation. 1979; 60: 1156-1160.
45. Davidson et al. Measurement of Tidal Volume by Using Transthoracic Impedance Variations in Rats. J Appl Physiol. 1999; 86: 759 - 766.
46. Peacock IV et al. Bioimpedance Monitoring: Better Than Chest X-Ray for Predicting Abnormal Pulmonary Fluid? Congestive Heart Failure. 2000; 6(2): 86-89.
47. Campos et al. Functional Valvular Incompetence in Decompensated Heart Failure: Noninvasive Monitoring and Response to Medical Management. Am J Med Sci. 2005; 329(5): 217-21.
48. Zlochiver et al. Monitoring lung Resistivity Changes in Congestive Heart Failure Patients Using the Bioimpedance Technique. Congest Heart Fail. 2005; 11(6):289-93
49. David A. Nierman, Jeffrey I. Mechanick. Evaluation of Transthoracic Bioelectrical Impedance Analysis in Monitoring lung Water During Diuresis. Applied Cardiopulmonary Pathophysiology 1998; 7: 57-62.
50. Cheuk-Man Yu et al. Intrathoracic Impedance Monitoring in Patients With Heart Failure: Correlation With Fluid Status and Feasibility of Early Warning Preceding Hospitalization. Circulation. 2005; 112: 841-848.
51. Spinale et al. Noninvasive Estimation of Extravascular Lung Water Using Bioimpedance. Journal of Surgical Research. 1989; 47: 535-540.
52. Wang et al. Feasibility of Using an Implantable System to Measure Thoracic Congestion in an Ambulatory Chronic Heart Failure Canine Model. PACE. 2005; 28: 404-411
53. Newman et al. Thoracic-Fluid Conductivity in Peripartum Women with Pulmonary Edema. Obstet Gynecol. 1999; 94: 48-51
54. Zerahn et al. The Effect of Thoracentesis on lung Function and Transthoracic Electrical Bioimpedance. Respir Med. 1999; 93(3): 196-201
55. Raaijmakers et al. Estimation of Non-cardiogenic Pulmonary Oedema Using Dual-Frequency Electrical Impedance. Med. Biol. Eng. Comput. 1998; 36: 461-466.

56. Packer et al. Utility of Impedance Cardiography for the Identification of Short-Term Risk of Clinical Decompensation in Stable Patients with Chronic Heart Failure. J Am Coll Cardiol. 2006; 47:2245-2252.
57. LW. Stevenson, JK. Perloff. The Limited Reliability of Physical Signs for Estimating Hemodynamics in Chronic Heart Failure. JAMA. 1989; 261: 884-8.
58. Bioimpedance Analysis Laboratory of the Body Composition Unit of the New York Obesity Research Center at St. Luke´s-Roosevelt Hospital. (http://www.nyorc.org/bcu/labs/bioimpedence.html).
59. Nohria et al. Evaluation and Monitoring of Patients with Acute Heart Failure Syndromes. Am J Cardiol. 2005; 96[suppl]: 32G-40G.
60. ESCAPE Investigators. Evaluation Study of Congestive Heart Failure and Pulmonary Artery Catheterization Effectiveness (ESCAPE Study). JAMA. 2005; 294: 1625-33.
61. Kathryn Truter Von Rueden. Outpatient Hemodynamic Monitoring of Patients with Heart Failure. Journal of Cardiovascular Nursing. 2002; 6 (3): 62(10).
62. Belardinelli et al. Comparison of Impedance Cardiography with Thermodilution and Direct Fick Methods for Noninvasive Measurement of Stroke Volume and Cardiac Output During Incremental Exercise in Patients with Ischemic Cardiomyopathy. Am J Cardiol. 1996; 77(15):1293-301.
63. Shoemaker et al. Multicenter Trial of a new Thoracic Electrical Bioimpedance Device for Cardiac Output Estimation. Crit Care Med. 1994; 22(12):1907-12.
64. Raisinghani et al. The COST study: A Multicenter Trial Comparing Measurement of Cardiac Output by Thoracic Electrical Bioimpedance with Thermodilution. American College of Cardiology 47th Annual Scientific Sessions, April 1, 1998.
65. Wang et al. Impedance Cardiography: More Questions than Answers (abstract). Current Heart Failure Reports. 2006; 3: 107-113.
66. Peng et al. An Investigation to show the Effect of Lung Fluid on Impedance Cardiac Output in the Anaesthetized Dog. British Journal of Anaesthesia. 2005 95(4):458-464.
67. W. Sageman, D. Amundson. Thoracic Electrical Bioimpedance Measurement of Cardiac Output in Postaortocoronary Bypass Patients. Crit Care Med. 1993; 21(8):1139-42.
68. Doering et al. Predictors of Between-method Difference in Cardiac Output Measurement using Thoracic Electrical Bioimpedance and Thermodilution. Crit Care Med. 1995; 23(10):1667-73.

69. Alt et al. Feasibility of Using Intracardiac Impedance Measurements for Capture Detection. PACE.1992; 15 (11): 1873.
70. Alt et al. Control of Pacemaker Rate by Impedance-based Respiratory Minute Ventilation. Chest. 1987; 92: 247-252.

9. Appendix

Abbreviations

ACE – angiotensin converting enzyme

AD – analog to digital

AHA – American Heart Association

AMI – acute myocardial infarction

ASS – acetyl salycic acid (Aspirin®)

BNP – B- type natriuretic peptides

BR – breath rate

BW – body weight

CAD – coronary artery disease

CCO – continuous cardiac output

CHD – coronary heart disease

CHF – congestive heart failure

CO – cardiac output

CO_2 - carbon dioxide

CS – coronary sinus

CVP – central venous pressure

dP/dT – delta pressure / delta time

ECG - electrocardiogram

ECG-LVH – electrocardiographic left ventricular hypertrophy

ECV – extra cellular volume

ESCAPE Study – Evaluation Study of Congestive Heart Failure and Pulmonary Artery Catheterization Effectiveness (ESCAPE Study).

fl1 – first fluid overload stage

fl2 – second fluid overload stage

HES – hydroxethyl starch

HF – heart failure

IE – units

IM – intra muscular

IV – intra venous

KHK – Koronarherzkrankheit (coronary heart disease)

kHz – kilo Hertz

kg - kilogram

LV – left ventricle (or left ventricular)

LVEDP – left ventricular end diastolic pressure

LVEDZ – left ventricular end diastolic impedance

LVESP – left ventricular end systolic pressure

LVESZ – left ventricular end systolic impedance

mg – milligram

ml – milliliter

MI - myocardial infarction

mmHg - millimetres of mercury

MPAP – mean pulmonary artery pressure

Ω - ohm

O_2 – oxygen

PAP – pulmonary artery pressure

PCWP – pulmonary capillary wedge pressure

PDE5 - 5-phosphodiesterase

PNP - paroxysmal nocturnal dyspnea

PSA – pacing system analyser

RA – right atria

RV – right ventricles

RVEDP – right ventricular end diastolic pressure

S3 – third heart sound

SubQ arrays – subcutaneous arrays

SV – stroke volume

TV – tidal volume

Z – bioimpedance, impedance

List of Figures

List of Tables

Acknowledgements

Special thanks go to my supervisor **Dr. Parwis Fotuhi** for the success of this thesis work. His availability from the very beginning to the end made problem solving quick and uncircumstancial. His efforts made it possible for me to go to the USA to do this research work. His contributions to problem identification, openness for discussions at any time, his invaluable comments, criticisms and suggestions led to the success of my thesis research. His help was not only scientific; he was more than a supervisor: a mentor and a friend.

I am grateful to **Prof. Dr. Eckhardt Alt** for providing me with the necessary materials, space and advice required through out my thesis research. His kindness made the stay in New Orleans very friendly.

I am very grateful to the **Alliance of Cardiovascular Researchers** for the financial support.

Todd Luka for modifying the Labview program to ease data analysis, his efforts in solving computer problems as well as his readiness to discuss and solve problems and his important suggestions and comments. His cheerful nature also had a great input in easing a stressed mind.

Walter Mildenberger for his advice and support by the data analysis.

Christian Valina for his work especially with the animal experiments and his friendly advice.

Kai Pinkernel for his advice and help in problem situations.

Chrisoph Nabzdyk, **Roman Schlager** and **Peter Wrede** for those sleepless nights of going through the Data, and a fantastic working and living environment. I would also like to thank the entire laboratory personnel of Dr. Alt's lab for their help and co-operation during my working and research there. My genuine thanks go to my friends **Charity Mutegi** and **Til Kiderlen** for proof reading the final version of the thesis and for the useful comments and suggestions they gave me to make the thesis clearly readable and easily understandable.

I would like to thank my Family: My parents **Rebecca Mutwol** and **Francis Mutwol**, and my brothers and sisters for their moral support and making all this possible. Last but not least I would like to thank **Dorcas Komen, Nicole Zepmeisel** and all my friends who supported me directly or indirectly during the course of this work.

This research work was carried out between April 2004 and March 2005 at Tulane University Health Sciences Center in New Orleans, Louisiana, USA.

Curricilum Vitae

Mein Lebenslauf wird aus datenschutzrechtlichen Gründen in der elektronischen Version meiner Arbeit nicht veröffentlicht**.**

Erklärung

Ich, Lawrence Mutwol, erkläre an Eides statt, dass ich die vorgelegte Dissertationsschrift mit dem Thema “A Novel Method of Early Detection of Congestion in Heart Failure Using Bioimpedance on a Pig Model” selbst verfasst und keine anderen als die angegebenen Quellen und Hilfsmittel benutzt, ohne die (unzulässige) Hilfe Dritter verfasst und auch in Teilen keine Kopien anderer Arbeiten dargestellt habe.

Berlin, Datum
Lawrence Mutwol.